

**STRENGTHENING OF REINFORCED CONCRETE FRAME
USING AN ECCENTRIC WALL**

by

Larry Roland Jimenez

THESIS

**Presented to the Faculty of the Graduate School of
The University of Texas at Austin
in Partial Fulfillment
of the Requirements
for the Degree of**

MASTER OF SCIENCE

THE UNIVERSITY OF TEXAS AT AUSTIN

May 1989

ACKNOWLEDGEMENTS

This Research project was Funded by The National Science Foundation Grant ECE- 8416147, "Strengthening of Reinforced Concrete Frame Structures". I wish to express my gratitude to Dr. James O. Jirsa for his invaluable direction and counsel of this project. Special thanks to Dr. Michael E. Kreger for his advice and support provided. My gratitude to Loring Wyllie of Degenkolb Associates , San Francisco, for his contribution to this project.

Implementation of this project was made possible by the unconditional help of the Ferguson Laboratory Staff. Special thanks to Dick Marshall, Blake Stasney, Pat Ball, Robert Garcia, Wayne Little, Alec Tahmessebi, Laurie Golding, Irene Moore, Maxime DeButts, Sharon Cunningham, and Jean Gehrke.

I would like to give thanks to all my fellows in Ferguson Lab., in special to Rodrigo Jordan, Sanjeev Shah, Hakim Bouadi, Sergio Alcocer, Ed Breeze and Enrique Martinez for their contributions in the construction and testing phases of this project.

I am grateful to the Agency for The International Development (USAID) for its moral and financial support, without its help it wouldn't be possible to achieve this project. My most sincere gratitude to Franz Sauter, my master, friend and model, thank you for encouraging me in this campaign. Finally, to those who always were with me when I needed them most, to God and my family, thank you for giving me the chance to live.

ABSTRACT
STRENGTHENING OF REINFORCED CONCRETE FRAME
USING AN ECCENTRIC WALL

by

LARRY ROLAND JIMENEZ

SUPERVISING PROFESSOR: JAMES O. JIRSA

The performance of a non-ductile reinforced concrete frame strengthened with a reinforced concrete wall designed to carry inplane lateral cyclic loads was investigated. A two-third scale model was built and tested. The reinforced concrete frame was representative of 1950's construction in seismic areas. The frame columns had a compression splice at the base of the columns. In previous tests, a splice failure occurred in the columns when the boundary element was in tension. The splice failure limited the capacity of this strengthened frame system. In the current test, the concrete wall was eccentric to the plane of the frame. It was connected to the concrete frame through epoxy grouted dowels and reinforced concrete jackets around the frame columns and was faced against the outside of the columns. The jackets improved the behavior of the column splice, allowing steel strains well beyond yield without failing. The vertical wall and column reinforcement at the base was well into the yield range and the load-deflection curve was nearly flat indicating that the ultimate load in flexure was almost reached. The capacity reached at the end of the test was higher than the maximum strength predicted by ACI 318-86.

TABLE OF CONTENTS

	<u>Page</u>
CHAPTER 1	1
1.1 Objective	1
1.2 Background	1
1.2.1 Repair and retrofit of structure	1
CHAPTER 2	3
2.1 Introduction	3
2.2 Modelling of the Specimen	6
2.3 Design Criteria and Detailing	7
2.3.1 Existing frame	7
2.3.2 Strengthening element	9
2.4 Mechanical Characteristic of Materials	11
2.4.1 Concrete	11
2.4.2 Steel	12
2.4.3 Epoxy	12
2.5 Construction Procedure	12
2.5.1 General	12
2.5.2 Existing frame	14
2.5.3 Strengthening elements	16
2.6 Test Set-Up	21
2.6.1 General	21
2.6.2 Loading system	22
2.6.3 Data acquisition system	23

CHAPTER 3 - EXPERIMENTAL RESULTS	28
3.1 General	28
3.2 Response to Cyclic Loading	29
3.2.1 Cycles to 150 kips	31
3.2.2 Cycles to 0.1% Drift [cycles 7 and 8]	32
3.2.3 Cycle to 0.2% Drift [cycles 9, 10 and 11]	35
3.2.4 Cycle to 0.3% Drift [cycle 12]	37
3.2.5 Cycle to 0.4% Drift [cycle 13]	39
3.2.6 Cycle to 0.6% Drift [cycle 14]	41
3.3 Column Splice	42
3.4 Shear Connector Dowels	43
CHAPTER 4 - EVALUATION OF EXPERIMENTAL RESULTS	45
4.1 Lateral Displacement Response	45
4.1.2 Theoretical lateral stiffness	45
4.2.3 Measured lateral stiffness	46
4.2 Deflection Components	47
4.3 Prediction of Strength	51
4.3.1 Flexural cracking strength	51
4.3.2 Flexural strength	52
4.3.2.1 Analysis using ACI code assumptions	52
4.3.2.2 Refined analysis	53
4.3.3 Shear strength	55
4.3.4 Splice design	57
4.4 Energy Dissipation Capacity	57
4.5 Comparison of Eccentric Wall to Infill Wall	59

CHAPTER 5 - SUMMARY, CONCLUSIONS AND RESEARCH	
RECOMMENDATIONS	64
5.1 Summary	64
5.2 Conclusions	64
5.3 Research Recommendations	65
REFERENCES	66

LIST OF TABLES

	<u>Page</u>
2.1 Concrete mix proportions per batch	11
2.2 Concrete strength (psi)	11
2.3 Epoxy Resin Specification Data	12
4.1 Strength Evaluation	56

LIST OF FIGURES

		<u>Page</u>
2.1	Failures of Splice Infill Wall (Gaynor)	4
2.2	Proposed Strengthening Scheme	5
2.3	Existing Frame Reinforcement Layout	6
2.4	Foundation Girder Layout	8
2.5	Shear Dowel Detail	10
2.6	Experimental Strain-Stress Relationships of Reinforcement	13
2.7	Frame Formwork	14
2.8	Vertical Positioning of Bounding Frame	15
2.9	Foundation Girder Prior to Casting	16
2.10	Column Splice Before Casting	17
2.11	Column Splice After Casting	18
2.12	Boundary Element-Transverse Reinforcement in Column Region	19
2.13	Boundary Element-Transverse Reinforcement in Top Beam Region	19
2.14	Wall and Encasing Reinforcement as Built	20
2.15	Typical Formwork Assembly	21
2.16	Strengthening Element Casting Operation	22
2.17	Loading Assembly Set-Up	24
2.18a	Strain Gages Location	25
2.18b	Strain Gages Location	26
2.19	Deflection Transducer Locations	27
3.1	Load History	28
3.2	Drift History	29
3.3	Measured Load-Drift Response Curve	30

3.4	Ratio of Measured Secant Stiffness to Theoretical Elastic Stiffness	31
3.5	Energy Dissipated in each Cycle at Increasing Drift Levels	32
3.6	Crack Pattern at 150 kips (Loading North)	33
3.7	Crack Pattern at 150 kips (Loading South)	33
3.8	Crack Pattern at 0.1% Drift (Loading North)	34
3.9	Crack Pattern at 0.1% Drift (Loading South)	34
3.10	Crack Pattern at 0.2% Drift (Loading North)	36
3.11	Crack Pattern at 0.2% Drift (Loading South)	36
3.12	Steel-Strain Profile at the Base of the Wall (loading North) . . .	37
3.13	Steel-Strain Profile at the Base of the Wall (Loading South) . . .	38
3.14	Crack Pattern at 0.3% Drift (Loading North)	38
3.15	Crack Pattern at 0.3% Drift (Loading South)	39
3.16	Crack Pattern at 0.4% Drift (Loading North)	40
3.17	Crack Pattern at 0.4% Drift (Loading South)	40
3.18	Crack Pattern After Completion of the Test	41
3.19	Load-Strain Relationship Longitudinal Reinforcement in South Boundary Member	42
3.20	Load Strain Relationship Longitudinal Reinforcement in North Boundary Member	43
3.21	Load-Strain Relationship for Dowel Connectors (Loading North) .	44
3.22	Load-Strain Relationship for Dowel Connectors (Loading South) .	44
4.1	Theoretical Stiffness Variables	46
4.2	Ratio of Measured to Theoretical Stiffness vs. Load	47
4.3	Instrumentation for Determining Deflection Components	48
4.4	Fixed-End Rotation Effect	49
4.5	Lateral Deflection Components	50
4.6	Deflection Component Ratios	51

4.7	Notation for Flexural Analysis of Wall	53
4.8	Steel Strain-Stress Relationship Used in RCCOLA	54
4.9	Concrete Strain-Stress Relationship Used in RCCOLA	54
4.10	RCCOLA Moment-Curvature Relationship	55
4.11	Energy Dissipation in Each Cycle vs. Drift	58
4.12	Normalized Energy Dissipated on Each Cycle	58
4.13	Load vs. Drift Envelopes	60
4.14	Load vs. Normalized Stiffness	61
4.15	Energy Dissipated Per Cycle	62
4.16	Normalized Energy Dissipated in Each Cycle for Eccentric and Infill Walls	63

CHAPTER 1

1.1 Objective

The objective of this study was to determine the hysteretic behavior of a reinforced concrete frame strengthened by a reinforced concrete wall. A one- story, two-third scale model was built and tested. The response was evaluated in terms of stiffness, strength, ductility, and energy absorption capacity. The reinforced concrete frame was representative of 1950's design and construction practice in seismic zones. In previous tests [1,2], similar frames strengthened with infill walls demonstrated that a compression splice in the boundary column failed and limited the capacity of the strengthened frame. To prevent the splice failure, reinforced concrete column jackets were constructed along with the wall which was eccentric to the axis of the frame. No tests of eccentric walls have been reported in the literature.

1.2 Background

1.2.1 Repair and Retrofit of Structures. The experience gained regarding building damage and structural collapse in recent earthquakes, and improvements in understanding the response of structure to earthquake loads have resulted in significant changes in the design requirements. Analytical evaluation of the seismic safety of existing buildings has indicated that a large number of buildings constructed on the basis of previous codes need strengthening to satisfy current standards.

The strengthening may be preventive in the case of undamaged buildings. In the case of buildings that have suffered structural damage during an earthquake, repair and/or strengthening are needed. In some cases code regulations require strengthening if building use or occupancy is changed. The modified structure not only has to satisfy strength, but also serviceability requirements. Non-structural damage under moderate earthquakes and collapse of the structure under severe earthquakes must be prevented. Of particular importance are essential facilities such as hospitals, power and communication plants, and transportation facilities which must be operable after a severe earthquake.

Among the most common practices for strengthening/repair of reinforced concrete structures are; jacketing of columns [13], concentric or eccentric steel

braces [12], reinforced concrete piers [15], and reinforced concrete structural walls [1,2,11,12].

Reinforced concrete structural walls may provide high lateral capacity in a few elements. If those elements are conveniently located, they may allow the building to operate while it is being strengthened. Structural walls may be infill walls (framed into columns and beams), or eccentric walls (attached to the side face of a frame).

Infill walls are commonly connected to the boundary frame by mechanical connectors [11,12], or by epoxy grouted steel bars [1,2,11,12]. Any of the attachment techniques requires drilling holes in frame members, an activity that may require substantial effort considering the potentially unknown location of longitudinal and transverse reinforcement.

Mechanical connectors may fail in a brittle manner. Many designers recommend the use of epoxy grouted bars to avoid brittle failure. However, epoxy resins require extra care in handling and placing, especially in high temperature environments. Placing concrete in an infill wall may create some quality control problems, the most common one being the gap between the infill wall and the top floor beam [1,11,12]. From the performance point of view, previous tests on infill walls have shown that common failures are associated 1) with the concentration of shear at the top and bottom of the columns created by the concrete compression strut [11,12], 2) with detail deficiencies in the frames such as the case of compression splices acting in tension [1,2], and 3) to sliding shear along a horizontal plane defined by the end of dowels anchored into the wall.

In order to obtain the benefits of the structural walls, improve the construction quality, and minimize the adverse effects created by infill walls, the use of reinforced concrete eccentric walls with reinforced concrete jackets may provide a superior scheme of strengthening when compared with infill walls.

CHAPTER 2

2.1 Introduction

In previous tests Gaynor[1] and Shah[2] conducted experiments to determine the behavior of non-ductile reinforced concrete frames strengthened with infill walls. Gaynor's specimens consisted of three reinforced concrete frames, representative of 1950's design and construction, strengthened with shotcrete infill walls. Two third scale, one bay, one story frames were used in the experimental project. One of the specimens had a solid infill wall, while the other two had openings in the infill. Gaynor found that under reversed lateral loads, the strength of the specimen with the solid infill was limited by the failure of the boundary frame. A splice designed for compression at the base of the column failed in tension due to the overturning moment. An anchorage mode of failure is not ductile and is not desirable in the seismic resistant design where ductility is essential for developing energy absorption capacity in the structure. Figure 2.1 illustrates the observed column failure.

The current experimental program is an alternative solution to the infill technique used by Gaynor[1]. Working with the same prototype building, the current scheme, as shown in Figure 2.2, consisted of an eccentric reinforced concrete wall connected to the existing frame by a concrete jacket around the existing columns. Eccentric walls placed against the lateral surface of the frame elements are considered easier to build than infill walls, and their construction does not interfere with the building function. Jacketing of the columns improves the poor existing lateral reinforcement of the boundary elements and also works as an efficient mechanism to transfer loads from the existing frame to the eccentric wall. A failure of the splice at the base of the column was avoided by increasing the concrete cover and adding ties in the new jacket.

In order to make direct comparison with the solid infill wall tested by Gaynor[1], and to use the same test set-up, the dimensions and reinforcement of the frame were the same as Gaynor's test specimen.

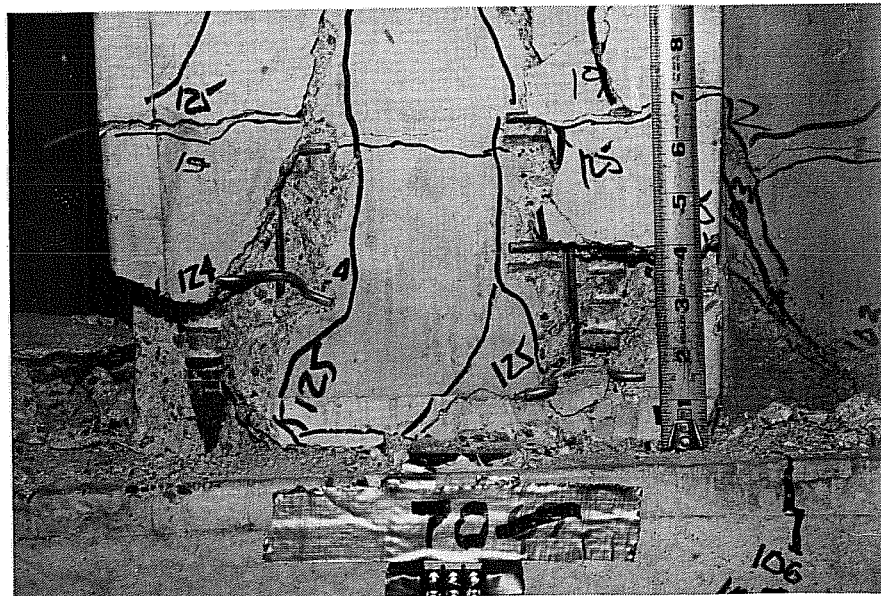
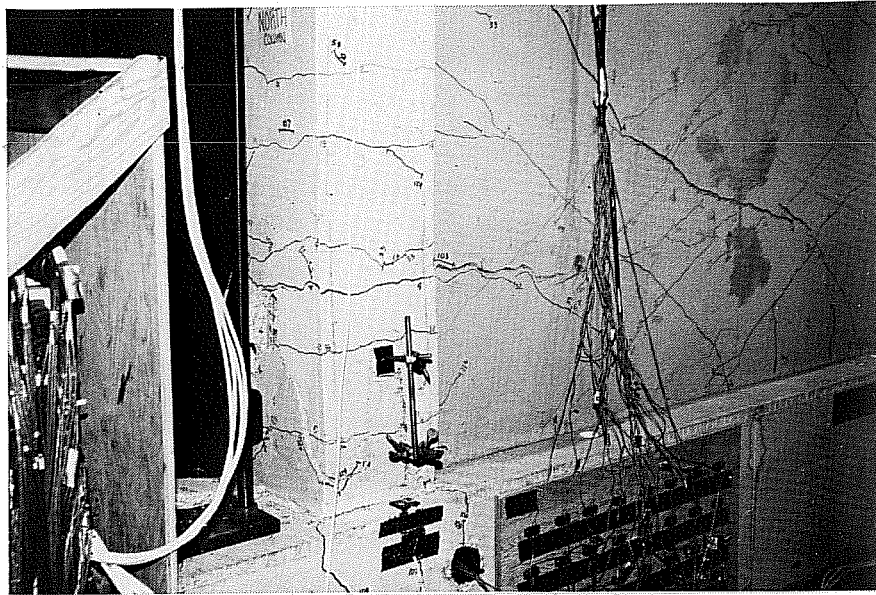


Figure 2.1 Failures of Splice in Infill Wall (Gaynor)

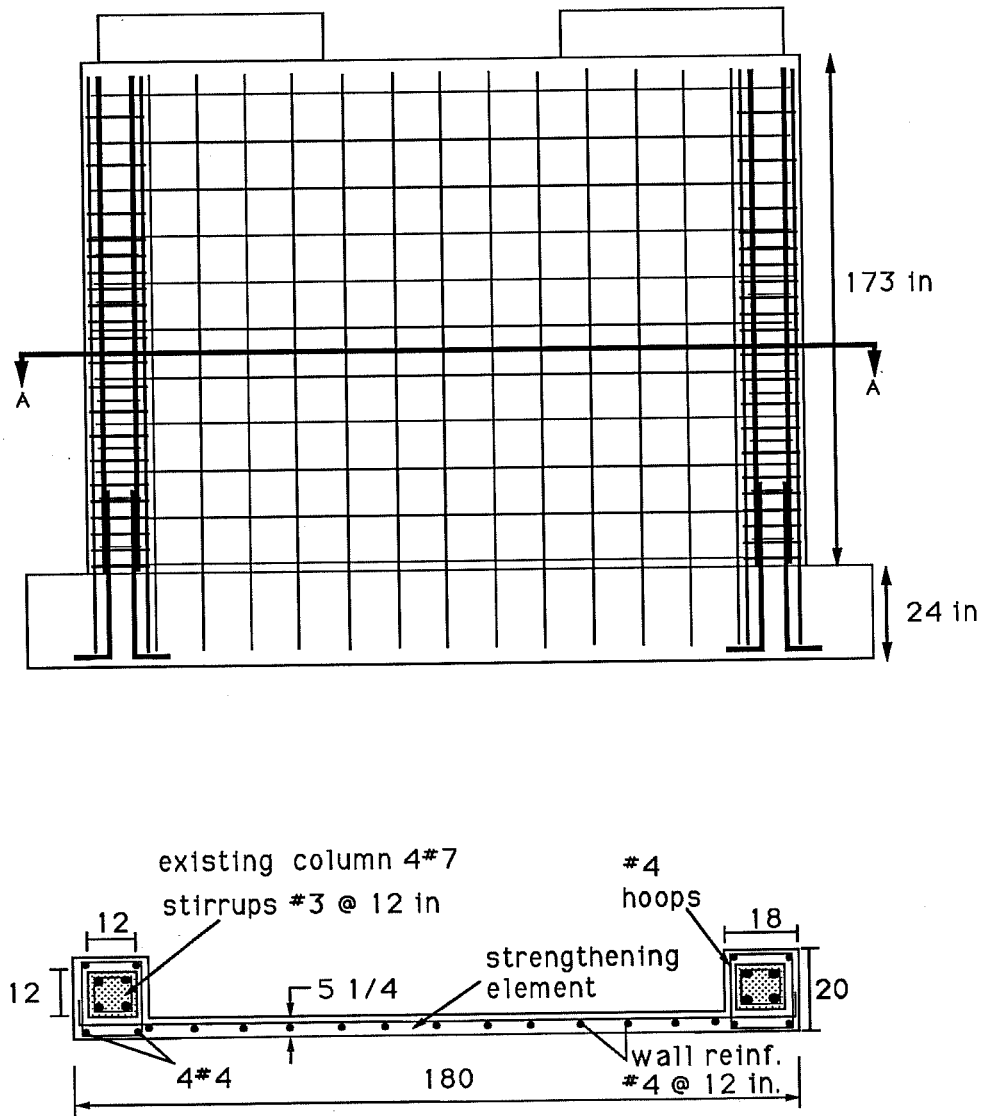


Figure 2.2 Proposed Strengthening Scheme

2.2 Modeling of the Specimen

The test model consisted of two elements, the “existing frame”, representing the prototype building to be strengthened, and the “strengthening element”, the new element added to improve the structural behavior of the building when subjected to earthquake loads.

The one bay existing frame, shown in Figure 2.3, was supported on a foundation girder. The lateral load was applied to the top beam through two loading blocks located at the top of the beam. Each block was capable of transferring half of the maximum shear expected in the test. The top beam had to be stiff and strong enough to distribute the shear uniformly throughout the specimen and function like a floor diaphragm in an actual structure. In addition, the bottom of the beam represented the floor beam of the prototype building in dimension and in the reinforcement.

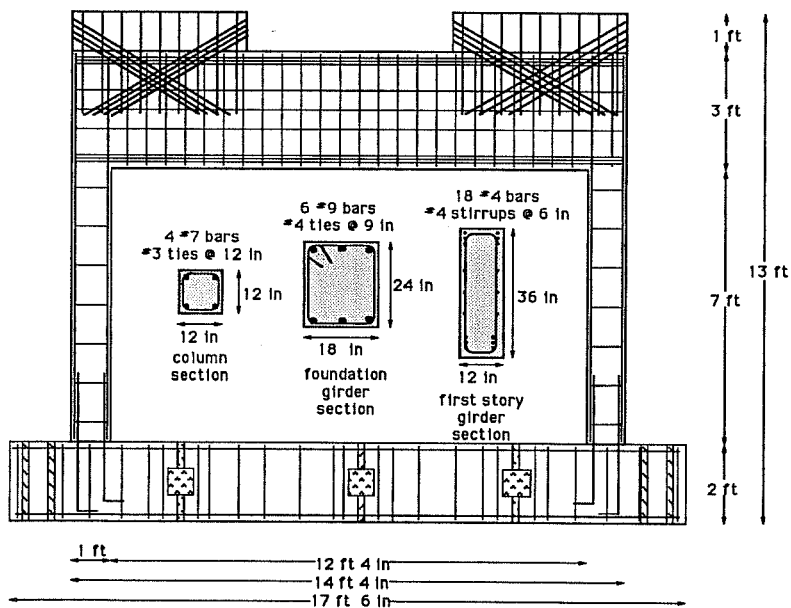


Figure 2.3 Existing Frame Reinforcement Layout

The foundation girder provided anchorage for the vertical reinforcement of the wall and columns. It was tied to the laboratory floor and represented a stiff foundation.

The strengthening element consisted of the structural wall and the column jackets. The jackets were built to increase the confinement of the boundary elements and to provide proper anchorage of the horizontal reinforcement of the wall into the boundary elements.

The transfer of shear from the existing frame to the new wall element was made through the column jackets and through epoxy grouted dowels embedded in the top beam in contact with the wall and at the bottom through bars anchored into the base beam.

Because the lateral load was applied concentric to the existing frame and eccentric to the wall, some torsion was expected. In a real building, the floor and roof diaphragms provide restraint to such induced torsion. To reproduce the diaphragm restraint, two steel braces were placed at the top of the specimen to limit the out of plane displacement of the wall.

2.3 Design Criteria and Detailing

2.3.1 Existing Frame. In order to make direct comparison with the full infill wall tested by Gaynor[1], it was decided not to change the geometry of the existing frame. The design of the existing frame is given in detail in reference [1].

In the design of the foundation girder, stresses induced by the reaction forces at the tiedown locations and loads produced in transportation of the girder were considered. The dimensions of the girder, 24 in. deep by 25 in. wide, were controlled by the minimum width required to give support to the boundary elements and the eccentric wall. Additional width facilitated placement of the formwork. The depth was kept as in previous tests to match with the test set-up used before. Minimum reinforcement controlled the longitudinal and transverse steel requirements.

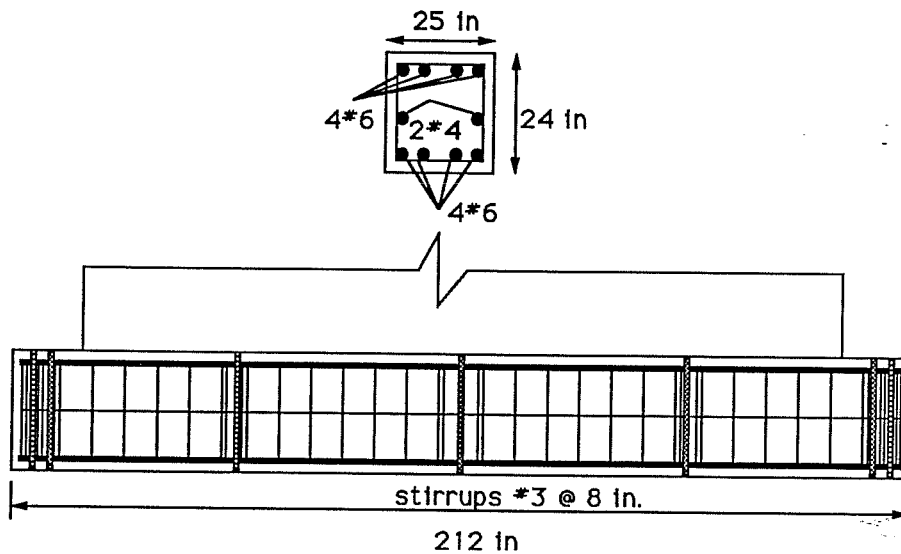


Figure 2.4 Foundation Girder Layout

Deformed #6 bars were used for the longitudinal steel and #3 bars for the hoops. Details of the reinforcement are illustrated in Figure 2.4.

The top girder was designed to transfer and distribute the shear to the wall. The amount of reinforcement was controlled by the concentration of stresses at the loading block region. The top beam depth was selected to increase the flexural moment to shear ratio at the base of the wall.

The columns were designed according to the ACI 318-56 code. Design forces were obtained from an analysis of a four story reinforced concrete frame prototype building subjected to lateral loads calculated according to the 1955 Uniform Building Code. Preliminary member sizes were 18 in. square columns, 12 by 18 in. floor beams, and a 6 in. thick solid concrete slab. Dead load included the self weight, a 20 psf partition load and 10 psf miscellaneous load. Live load was taken as 50 psf according to the 1955 UBC code. Loads were factored and moment coefficients were used to get maximum positive and negative beam moments. Column ties were #4 bars at the designated maximum spacing of 12 in.. Concrete strength of 4000 psi, and Grade 40 steel were taken as typical of the design values in the 1950's.

A two-thirds scale model was selected considering the laboratory space limitations and the lateral load capacity of the set-up. Under these conditions, a 1.5% column reinforced ratio was needed.

Detailing of the columns followed ACI 318-56 recommendations. The compression splice in the reinforcement at the base of the column and large spacing between stirrups were typical of the time.

2.3.2 Strengthening Element. The structural wall was designed following Appendix A of ACI 318-86. It was assumed that the existing frame and strengthening element behaved as a monolithic member. The influence of the aspect ratio was considered in the shear strength. Chapter 4 describes the design considerations. Grade 60 steel and 4000 psi. concrete were assumed in all the calculations.

Adequate ductility of the structure is one of the major concerns in seismic design. To meet that objective it was necessary to have flexural yielding of the wall before a shear failure occurred. A 5 1/4 in. thick concrete wall was identical to that tested by Gaynor[1]. Flexural capacity calculations did not take into account any axial load. In the most common cases, the axial load in structural walls falls below the balance point and increases the flexural capacity of the section. Flexural steel consisted of four #7 bars in each existing column, and four #4 bars in the concrete jacket. Minimum vertical reinforcement was used in the wall placed in a single curtain of #4 bars at 12 in. spacing in both directions.

A more refined flexural analysis was carried out with the computer program RCCOLA[5]. The purpose was to find the upper bound moment-curvature relationships for the wall using unconfined and confined sections. The stress-strain curve for the concrete followed the model proposed by Scott, Park and Priestley[7]. No axial load was considered.

Shear strength was computed according to code[3] recommendations. Minimum horizontal reinforcement (a single curtain of #4 bars at 12 in. spacing) was placed in the wall. Sliding shear was checked at the base of the wall considering a friction coefficient of 1.0.

In previous tests [1], it was found that the longitudinal reinforcement splice at the base of the existing column was not capable of developing the full strength of the bars and a non-ductile failure was produced. With this in mind, a reinforced

concrete jacket was designed to avoid the splice failure and to satisfy the transverse steel requirements for a tensile splice in the current code[3]. Following design guidelines of ACI Committee 408[4], the splice was checked using the cover and confining steel of the jacket. Minimum steel area at the maximum spacing, #4 bar hoops at a 4 in. spacing, were used and the spacing was reduced to 2 in. at the top and bottom of the boundary member. Figure 2.2 illustrates the reinforcement details of the strengthening element.

In order to transfer the shear force from the existing frame to the new element, epoxy grouted dowels were embedded in one side of the top beam. Deformed #6 hooked bars were designed to transfer the total shear using the shear friction provision in the code[3]. Although it was recognized that the new jackets were able to transfer part of the shear force, the contribution was neglected in design. Figure 2.5 illustrates the typical detail of the dowels.

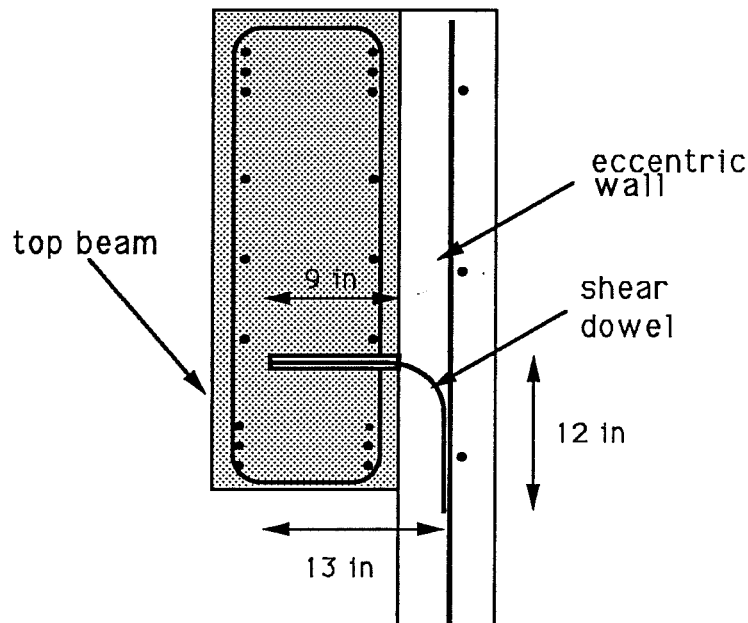


Figure 2.5 Shear Dowel Detail

Stresses due to the torsional moment, induced by the eccentricity of the wall before the braces provided out of plane restraint, were checked to prevent secondary damage and a possible early failure.

The foundation girder provided anchorage for the vertical reinforcement of the wall and columns. It was tied to the laboratory floor and represented a stiff foundation.

The strengthening element consisted of the structural wall and the column jackets. The jackets were built to increase the confinement of the boundary elements and to provide proper anchorage of the horizontal reinforcement of the wall into the boundary elements.

The transfer of shear from the existing frame to the new wall element was made through the column jackets and through epoxy grouted dowels embedded in the top beam in contact with the wall and at the bottom through bars anchored into the base beam.

Because the lateral load was applied concentric to the existing frame and eccentric to the wall, some torsion was expected. In a real building, the floor and roof diaphragms provide restraint to such induced torsion. To reproduce the diaphragm restraint, two steel braces were placed at the top of the specimen to limit the out of plane displacement of the wall.

2.3 Design Criteria and Detailing

2.3.1 Existing Frame. In order to make direct comparison with the full infill wall tested by Gaynor[1], it was decided not to change the geometry of the existing frame. The design of the existing frame is given in detail in reference [1].

In the design of the foundation girder, stresses induced by the reaction forces at the tiedown locations and loads produced in transportation of the girder were considered. The dimensions of the girder, 24 in. deep by 25 in. wide, were controlled by the minimum width required to give support to the boundary elements and the eccentric wall. Additional width facilitated placement of the formwork. The depth was kept as in previous tests to match with the test set-up used before. Minimum reinforcement controlled the longitudinal and transverse steel requirements.

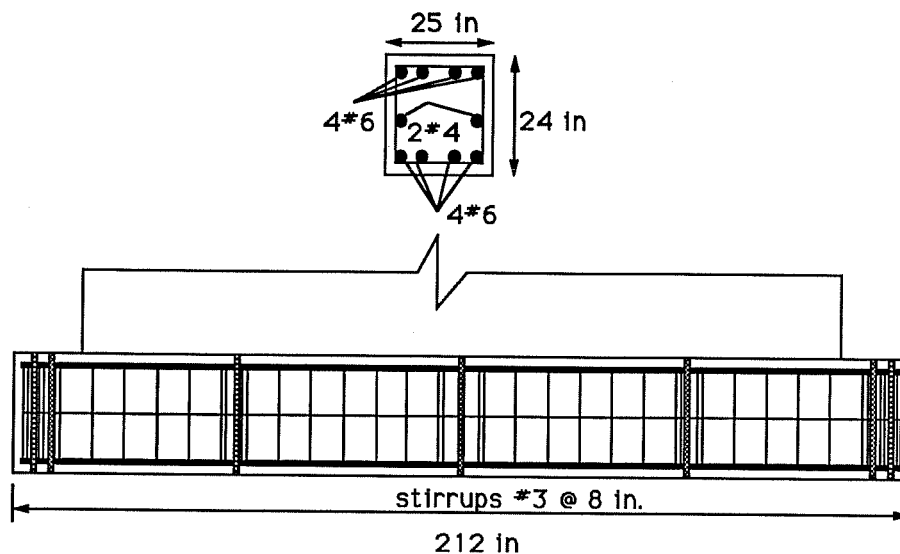


Figure 2.4 Foundation Girder Layout

Deformed #6 bars were used for the longitudinal steel and #3 bars for the hoops. Details of the reinforcement are illustrated in Figure 2.4.

The top girder was designed to transfer and distribute the shear to the wall. The amount of reinforcement was controlled by the concentration of stresses at the loading block region. The top beam depth was selected to increase the flexural moment to shear ratio at the base of the wall.

The columns were designed according to the ACI 318-56 code. Design forces were obtained from an analysis of a four story reinforced concrete frame prototype building subjected to lateral loads calculated according to the 1955 Uniform Building Code. Preliminary member sizes were 18 in. square columns, 12 by 18 in. floor beams, and a 6 in. thick solid concrete slab. Dead load included the self weight, a 20 psf partition load and 10 psf miscellaneous load. Live load was taken as 50 psf according to the 1955 UBC code. Loads were factored and moment coefficients were used to get maximum positive and negative beam moments. Column ties were #4 bars at the designated maximum spacing of 12 in.. Concrete strength of 4000 psi, and Grade 40 steel were taken as typical of the design values in the 1950's.

A two-thirds scale model was selected considering the laboratory space limitations and the lateral load capacity of the set-up. Under these conditions, a 1.5% column reinforced ratio was needed.

Detailing of the columns followed ACI 318-56 recommendations. The compression splice in the reinforcement at the base of the column and large spacing between stirrups were typical of the time.

2.3.2 Strengthening Element. The structural wall was designed following Appendix A of ACI 318-86. It was assumed that the existing frame and strengthening element behaved as a monolithic member. The influence of the aspect ratio was considered in the shear strength. Chapter 4 describes the design considerations. Grade 60 steel and 4000 psi. concrete were assumed in all the calculations.

Adequate ductility of the structure is one of the major concerns in seismic design. To meet that objective it was necessary to have flexural yielding of the wall before a shear failure occurred. A 5 1/4 in. thick concrete wall was identical to that tested by Gaynor[1]. Flexural capacity calculations did not take into account any axial load. In the most common cases, the axial load in structural walls falls below the balance point and increases the flexural capacity of the section. Flexural steel consisted of four #7 bars in each existing column, and four #4 bars in the concrete jacket. Minimum vertical reinforcement was used in the wall placed in a single curtain of #4 bars at 12 in. spacing in both directions.

A more refined flexural analysis was carried out with the computer program RCCOLA[5]. The purpose was to find the upper bound moment-curvature relationships for the wall using unconfined and confined sections. The stress-strain curve for the concrete followed the model proposed by Scott, Park and Priestley[7]. No axial load was considered.

Shear strength was computed according to code[3] recommendations. Minimum horizontal reinforcement (a single curtain of #4 bars at 12 in. spacing) was placed in the wall. Sliding shear was checked at the base of the wall considering a friction coefficient of 1.0.

In previous tests [1], it was found that the longitudinal reinforcement splice at the base of the existing column was not capable of developing the full strength of the bars and a non-ductile failure was produced. With this in mind, a reinforced

concrete jacket was designed to avoid the splice failure and to satisfy the transverse steel requirements for a tensile splice in the current code[3]. Following design guidelines of ACI Committee 408[4], the splice was checked using the cover and confining steel of the jacket. Minimum steel area at the maximum spacing, #4 bar hoops at a 4 in. spacing, were used and the spacing was reduced to 2 in. at the top and bottom of the boundary member. Figure 2.2 illustrates the reinforcement details of the strengthening element.

In order to transfer the shear force from the existing frame to the new element, epoxy grouted dowels were embedded in one side of the top beam. Deformed #6 hooked bars were designed to transfer the total shear using the shear friction provision in the code[3]. Although it was recognized that the new jackets were able to transfer part of the shear force, the contribution was neglected in design. Figure 2.5 illustrates the typical detail of the dowels.

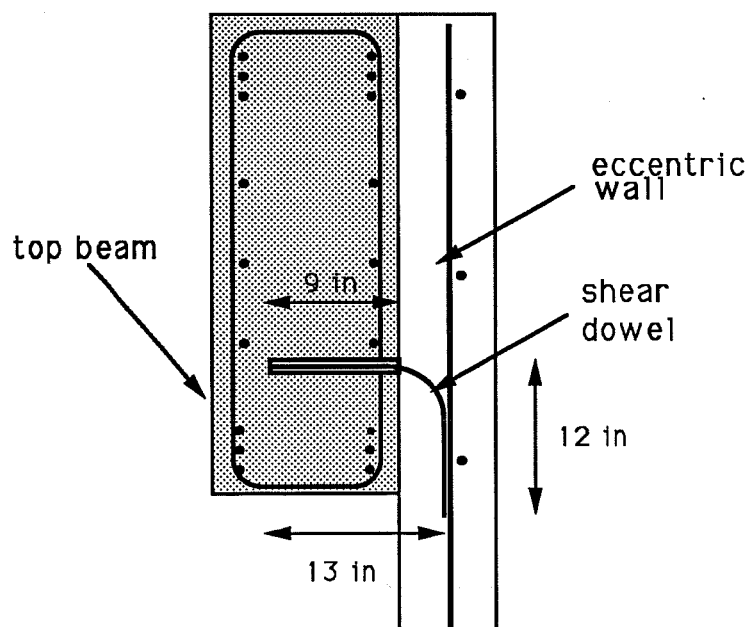


Figure 2.5 Shear Dowel Detail

Stresses due to the torsional moment, induced by the eccentricity of the wall before the braces provided out of plane restraint, were checked to prevent secondary damage and a possible early failure.

2.4 Mechanical Characteristics of Materials

2.4.1 *Concrete.* The nominal concrete strength at 28 days was 4000 psi for the elements in the specimen. Ready mix concrete was used for the different stages of construction. The maximum size of the coarse aggregate was 3/8 in. for ease of casting considering the congestion of steel in some regions and the small clearances within the formwork. Mix proportions for each batch are shown in Table 2.1. Standard 6 by 12 in. cylinders were cast and tested at seven, twenty-eight days, and on the date of test. Results of tests are presented in Table 2.2.

Table 2.1
Concrete mix proportions per batch

Element	Cement	Sand	Coarse Aggregate	Water
	(lb)	(lb)	(lb)	(lb)
Existing frame	471	1751	1625	279
Foundation girder	1902	7030	7000	480
Splice joint	1400	5320	6520	600
Wall and encasing	2118	7880	7320	675

Table 2.2
Concrete strength (psi)

Element	at 7 days	at 28 days	at test
Existing frame	2950	3550	4200
Foundation girder	4240	4400	4750
Splice joint	4250	4300	5300
Wall and encasing	3700	4130	4500

A superplasticizer additive (MB400N water-reducing admixture by Master Builders) was used. Twelve ounces of additive per one hundred pounds of cement was added to the batch used to cast the wall and column jackets. The slump was increased from 3 to 7 in.. The rest of the concrete was cast with a 4 in. slump.

2.4.2 Steel. Deformed Grade 60 bars were used. Although Grade 40 was common in 1950's construction, Grade 40 was not readily available. Stress-strain curves were obtained for the different bar sizes, and shown in Figure 2.6.

2.4.3 Epoxy. A two component, non-sag epoxy gel, Concessive Paste (LPL) by Master Builders, was used to grout the steel into the top beam. Table 2.3 shows the manufacture specifications for the epoxy gel.

Table 2.3
Epoxy Resin Specification Data

Tensile Strength	1,500 psi (10.3 MPa)
Elongation at Break (ASTM D 638)	4%
Compressive Yield Strength	8,000 psi (55.2 MPa)
Compressive Modulus (ASTM D 695)	4.0×10^5 psi (2.8×10^3 MPa)
Heat Deflection Temperature (ASTM D 648)	105°F (41°C)
Slant Shear Strength Damp-to-Damp Concrete (AASHTO T-237)	5,000 psi (34.5 MPa), 100% concrete failure

2.5 Construction Procedure

2.5.1 General. The specimen was built in three main stages; the foundation girder, the frame (top beam and columns), and the strengthening elements (structural wall and column jackets). Because the existing frame used by Gaynor[1] in the specimen with the full infill wall did not suffer much outside the region where the splice failed at the bottom of the column, it was decided to repair and reuse the

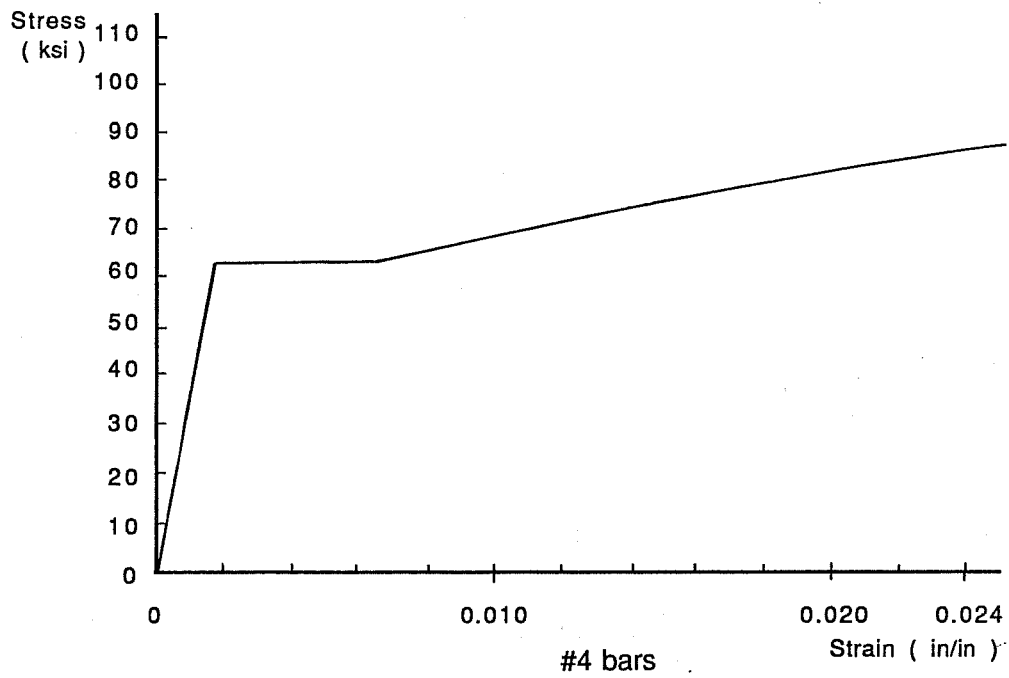
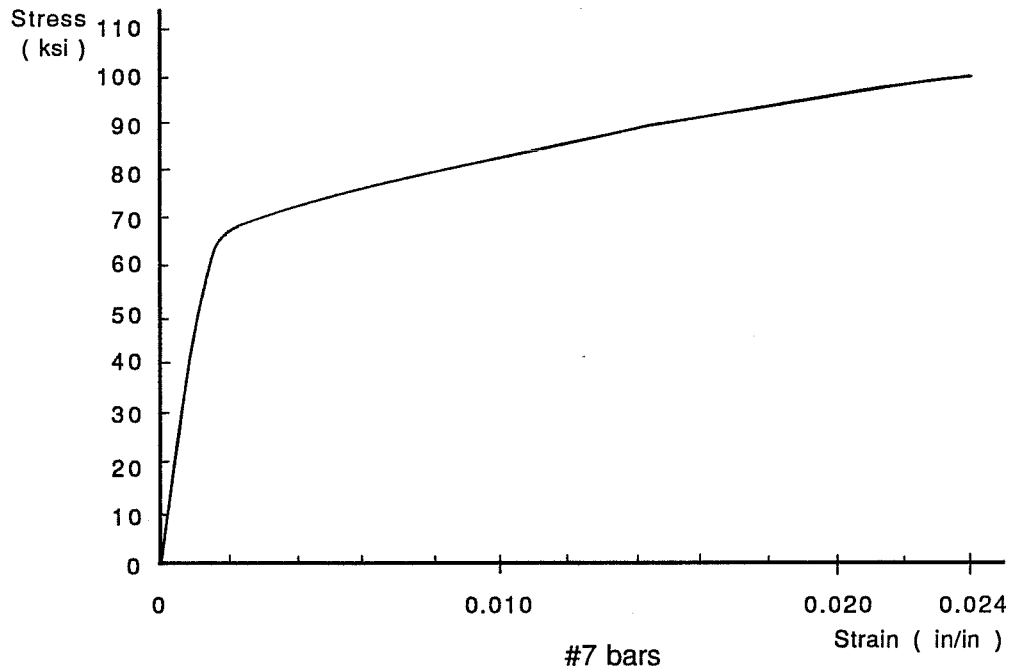


Figure 2.6 Experimental strain-stress relationships of reinforcement

frame to reduce the time of construction. A new foundation girder was required to provide a base for the new boundary members and eccentric wall.

2.5.2 Existing Frame. The existing frame was cast in a horizontal position for easy forming and concrete placement. The variation of the concrete strength over the height was considered to have negligible effect on the response. The formwork consisted of three platforms forming one side of the frame, and removable side forms bolted to the three platforms as illustrated in Figure 2.7. The entire frame was cast at the same time. Immediately after the concrete was placed, the exposed surface was covered with wet burlap and plastic to provide optimum curing conditions. Seven days later, the side forms were removed and the frame was lifted off the platforms with the overhead crane. The specimen was rotated into the upright position as shown in Figure 2.8. In Gaynor's test[1], the frame did not suffer significant damage as shown in Figure 2.1. After testing the solid shotcrete infill wall, the frame was moved and placed horizontally where the foundation girder and the infill wall were removed. The existing dowels used in the previous test were cut flush with the concrete surface.

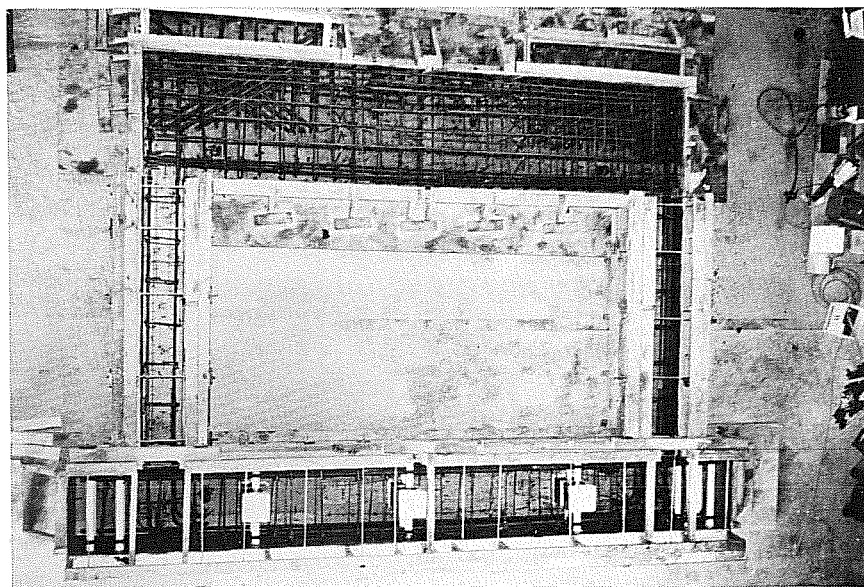


Figure 2.7 Frame Formwork

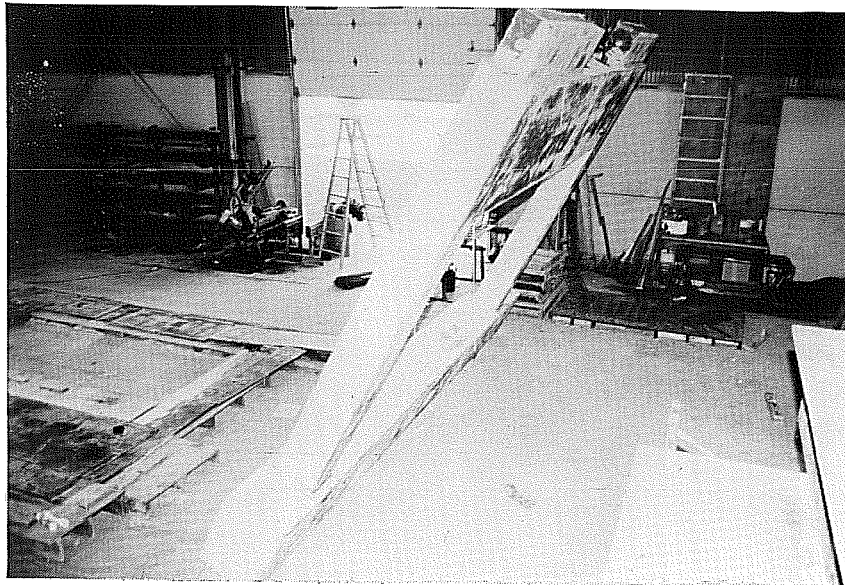


Figure 2.8 Vertical Positioning of Bounding Frame

A new foundation girder, 25 in. wide by 24 in. deep, was cast in its upright position. The vertical reinforcement of the wall was fully anchored in the girder as was the column reinforcement to be spliced. Figure 2.9 shows the foundation girder prior to casting.

Once the top part of the existing frame was ready, and the new foundation girder reached the concrete strength required for transportation, the girder was moved and placed in a horizontal position to make the splice. Accurate leveling was done to assure the alignment of the specimen during testing.

The damaged concrete from the previous test was removed from the original existing columns. It was considered that removal of the length of column 30 in. from the base was sufficient and would leave only sound concrete. In order to provide good bond between the old and new concretes, the surfaces were roughened with a chipping hammer. The loose concrete was removed with a steel brush, and free dust was vacuumed. Before casting, the surfaces were saturated with water for 24 hours to reduce shrinkage and promote bonding at the construction joint. Figures 2.10 and 2.11 illustrate the splice prior to and after the casting operation.

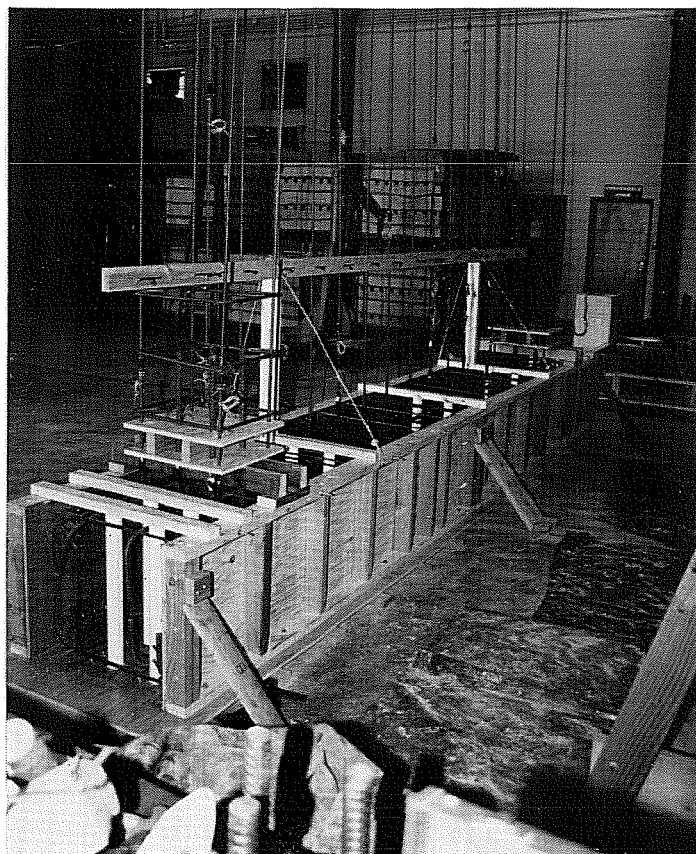


Figure 2.9 Foundation Girder Prior to Casting

2.5.3 Strengthening Elements. Seven days after the column splice was cast, the existing frame was lifted to an upright position and moved to the site where the structural wall was built.

The surfaces in contact with the strengthening elements were prepared to improve the bond between new and existing surfaces. With the help of power chipping hammers, up to 1/2 in. of the surface was removed to create a rough finish. The loose material was removed with a steel brush, and a jet air cleaning left the surface virtually free of dust.

The next step was to drill holes for the dowels and the confining stirrups in the top beam. One inch diameter by nine in. deep holes were drilled for the dowels. For the #4 stirrups, 5/8 in. diameter by 5 in. deep holes were prepared. The holes

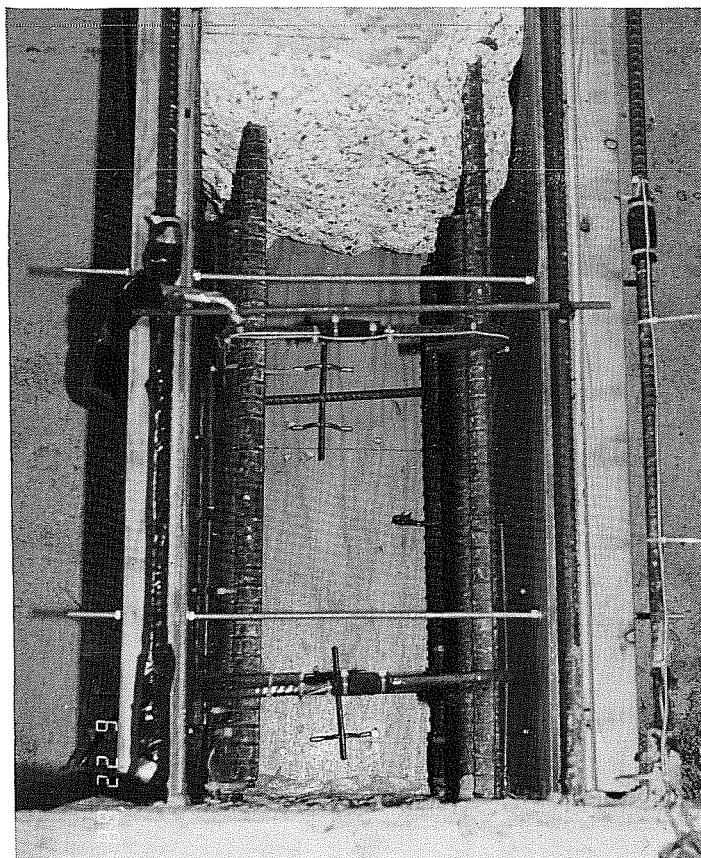


Figure 2.10 Column Splice Before Casting

were cleaned with a wire brush and vacuumed until they were virtually free of dust. The holes were then sealed with tape until the bars were grouted.

Before the grouting operation, the epoxy resin components were stored in a refrigerator for 10 hours to delay the time of setting after mixing. The components were mixed as directed with a mixer at 70° F room temperature. The epoxy mix was placed into disposable tubes and injected into the holes with a caulking gun. The tip of the nozzle was placed at the bottom of the hole and the caulking gun was slowly removed as the epoxy was placed. The bars were then placed into the hole with a twisting motion to expel any entrapped air. The grouting operation was done at 80° F temperature in the laboratory. Grouted bars were allowed to cure for several days before any further construction operations were started.

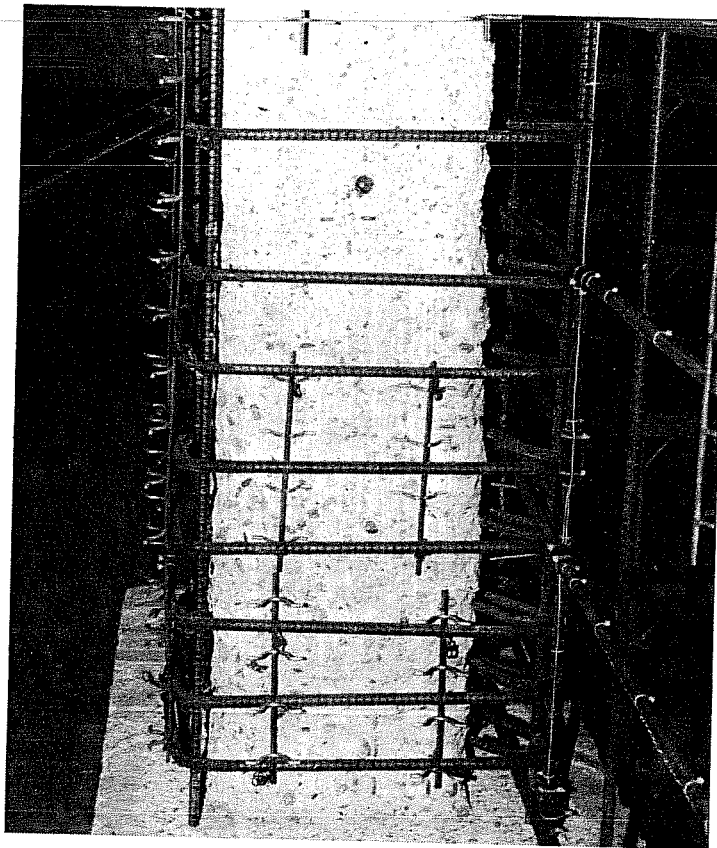


Figure 2.11 Column Splice After Casting

The new confining steel for the boundary elements consisted of two parts ties; a U-shaped open hoop and a cross tie completing the stirrup. Both parts were #4 bars ending in 135 degree hooks. For the column region above the bottom of the top beam, U-shaped #4 hoops were placed with the ends anchored into the top beam with epoxy grout. Figures 2.12 and 2.13 illustrate the details used.

The horizontal wall reinforcement was anchored with 90 standard hooks within the core of the new boundary element. Galvanized spacing chairs were used to control the position of the new reinforcement from the faces of the existing frame, and to provide the concrete cover specified. The final reinforcement layout is shown in Figure 2.14.

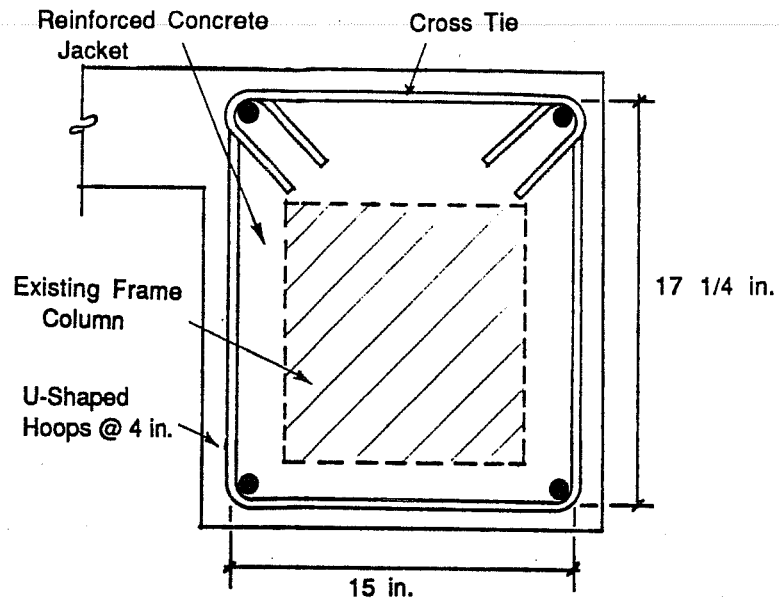


Figure 2.12 Boundary Element-Transverse Reinforcement in Column Region

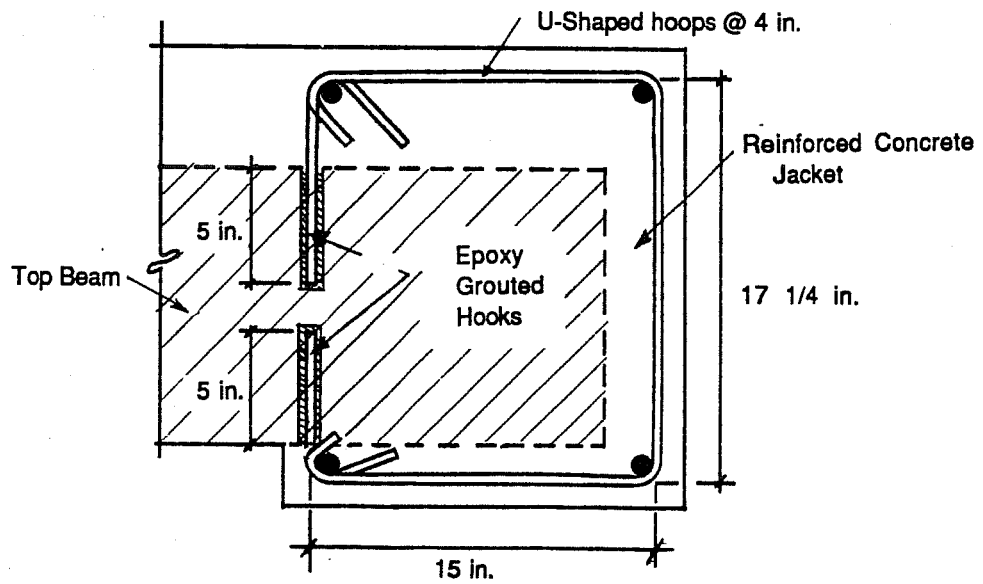


Figure 2.13 Boundary Element-Transverse Reinforcement in Top Beam Region

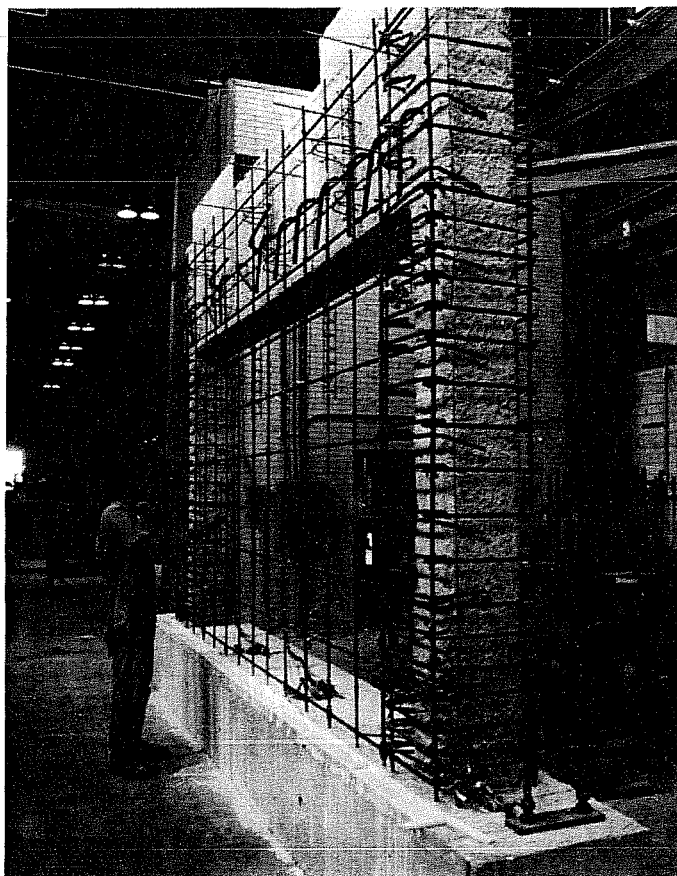


Figure 2.14 Wall and Encasing Reinforcement as Built

The formwork for the wall and jackets consisted of 3/4 in. plywood panels backed by 2 by 4 in. studs along the height of the wall and across the width of the columns. The studs were supported by wales spanning the entire width of the wall. Four lateral window openings, two in the wall and one in each column, were built at the midheight of the wall for vibrating the concrete and for observation of the concrete placement. Lateral wall pressures were self-equilibrated by tie rods through the wall. Over the region where the concrete wall was in contact with the top beam, the formwork panels were held in place using steel rods epoxy anchored in the beam. Precautions were taken to avoid the movement of the forms by attaching

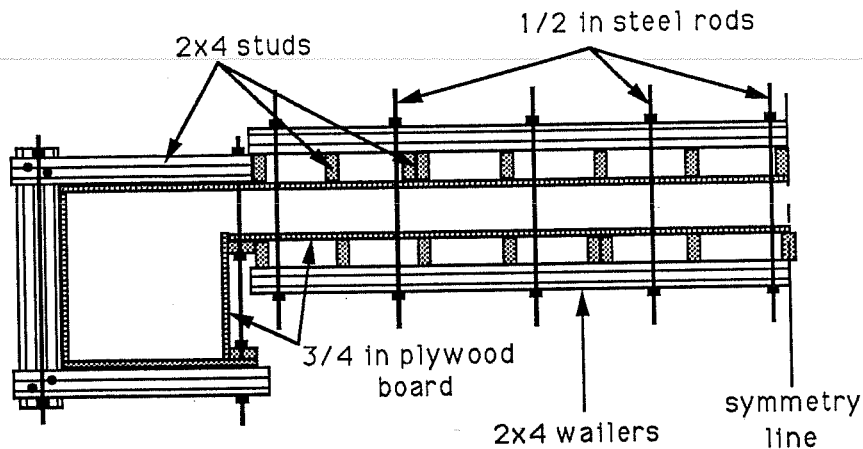


Figure 2.15 Typical Formwork Assembly

the forms rigidly to different points of the existing frame. A typical formwork section is illustrated in Figure 2.15.

All strengthening elements were cast in the same operation. The old concrete surfaces within the forms were wetted with water for 24 hours before casting to improve the bond between surfaces. The initial concrete slump was 3 in.. Maximum coarse aggregate size was $3/8$ in. The slump was increased to 7 in. by using a superplasticizer additive added after concrete arrived at the laboratory. The concrete was placed through the opening at the top of the wall with a one cubic yard bucket held by the overhead crane. Continuous vibration was provided through the midheight windows and from the top of the wall. Figure 2.16 shows the casting operation. The formwork was removed four days after casting and visual inspection of the surfaces did not reveal significant imperfections.

2.6 Test Set-Up

2.6.1 General. Ten days after the strengthening elements were cast, the specimen was moved to the testing site. The specimen was plumbed with steel plate shims. A $1/2$ in. space between the floor and the girder was filled with an expansive grout. Seven days later, when the grout reached 3500 psi strength, the specimen was

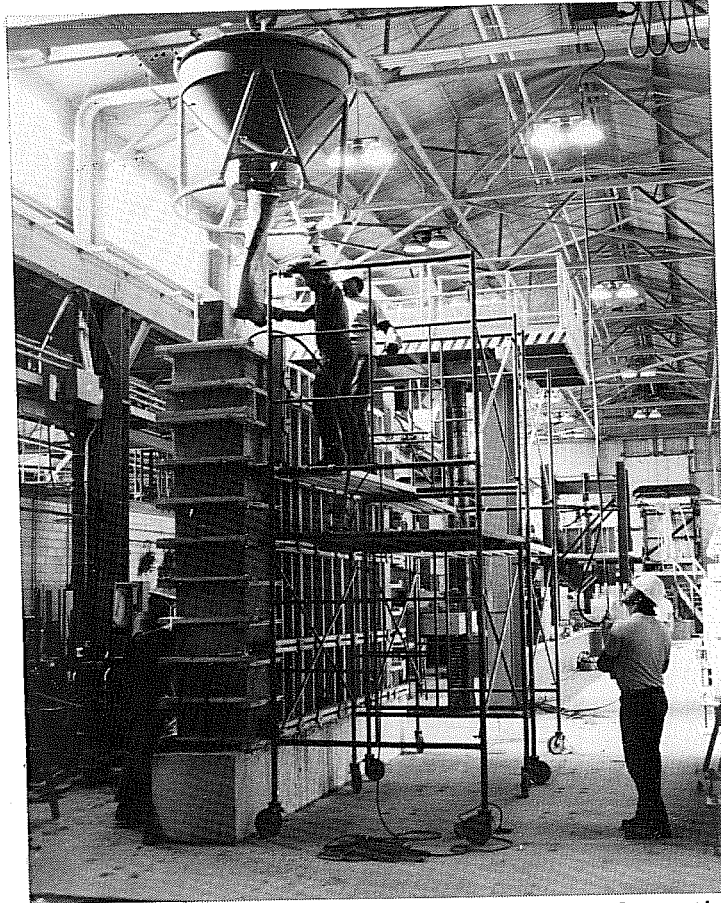


Figure 2.16 Strengthening Element Casting Operation

bolted to the reaction floor. Fourteen bolts were stressed to provide a total clamping force of 700 kips.

2.6.2 Loading System. Reversed cyclic lateral-in-plane loading was used to simulate the effects of earthquake ground motion. The loads were applied statically to the top of the specimen through the loading blocks. Four 100 ton hydraulic rams were used to apply the load. Only two rams were activated for loading in each direction. The idle rams were retracted while they were not in use. The rams reacted against the steel loading frame attached to the reaction wall. No axial load was applied during the test. Two steel braces were attached to the loading frame

to restrain out-of-plane displacement of the specimen due to torsion created by eccentricity between the applied load and the wall. Steel rods were placed between the loading blocks and the loading frame to prevent out-of-plane displacement of the specimen. Details of the assembly are illustrated in Figure 2.17.

The loading history was controlled by load increments up to the first observed shear crack, and by drift thereafter.

2.6.3 Data Acquisition System. Strain gages were placed on the reinforcement at critical sections of the specimen. Strains were measured in the existing frame and wall vertical reinforcement across several horizontal planes. Strains in the reinforcement was measured with gages placed along diagonal planes and where the wall horizontal reinforcement was anchored in the boundary members. Strains in the confining steel were also recorded in the old and new stirrups.

Seventy-four strain gages were placed as shown in Figure 2.18a and 2.18b. Gages were placed symmetrically to determine and compare the distribution of strain in both directions of loading.

Linear potentiometers were used to measure displacements at different locations. Lateral displacement due to flexure, shear, slip between existing and new interfaces, torsion, and those due to rigid body motion were considered. Twenty-two linear potentiometers were distributed as shown in Figure 2.19.

A pressure transducer was used to monitor the applied load. The load was determined from the hydraulic line pressure and the ram area. A pressure gage verified the readings of the transducer. Load and deflection was continuously monitored by an X-Y plotter.

An IBM-XT microcomputer was used to acquire the test data. The system converted voltages to engineering units. The number of scans per load cycle were selected to define the shape of the hysteresis curves. Hard copies of the scans were printed during the test. Progression of damage was recorded by photographs at important stages of loading.

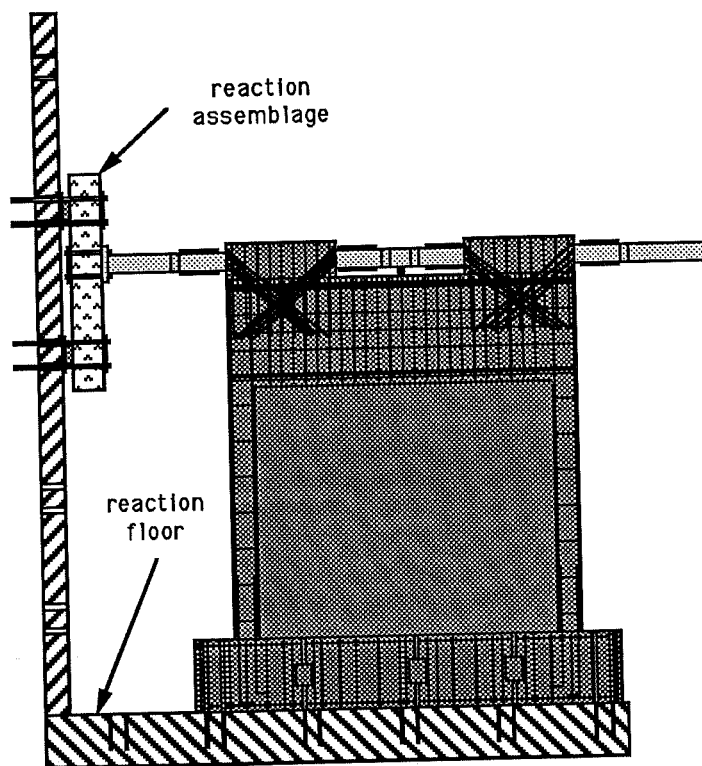
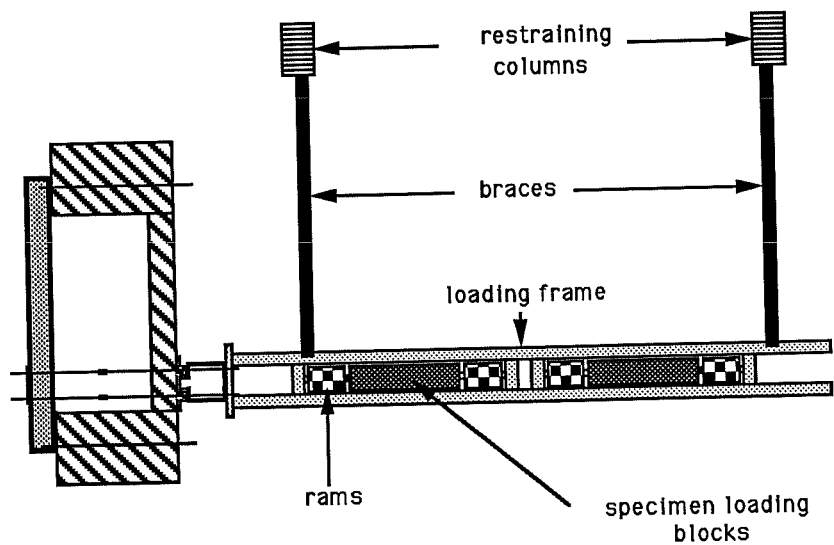


Figure 2.17 Loading Assembly Set-Up

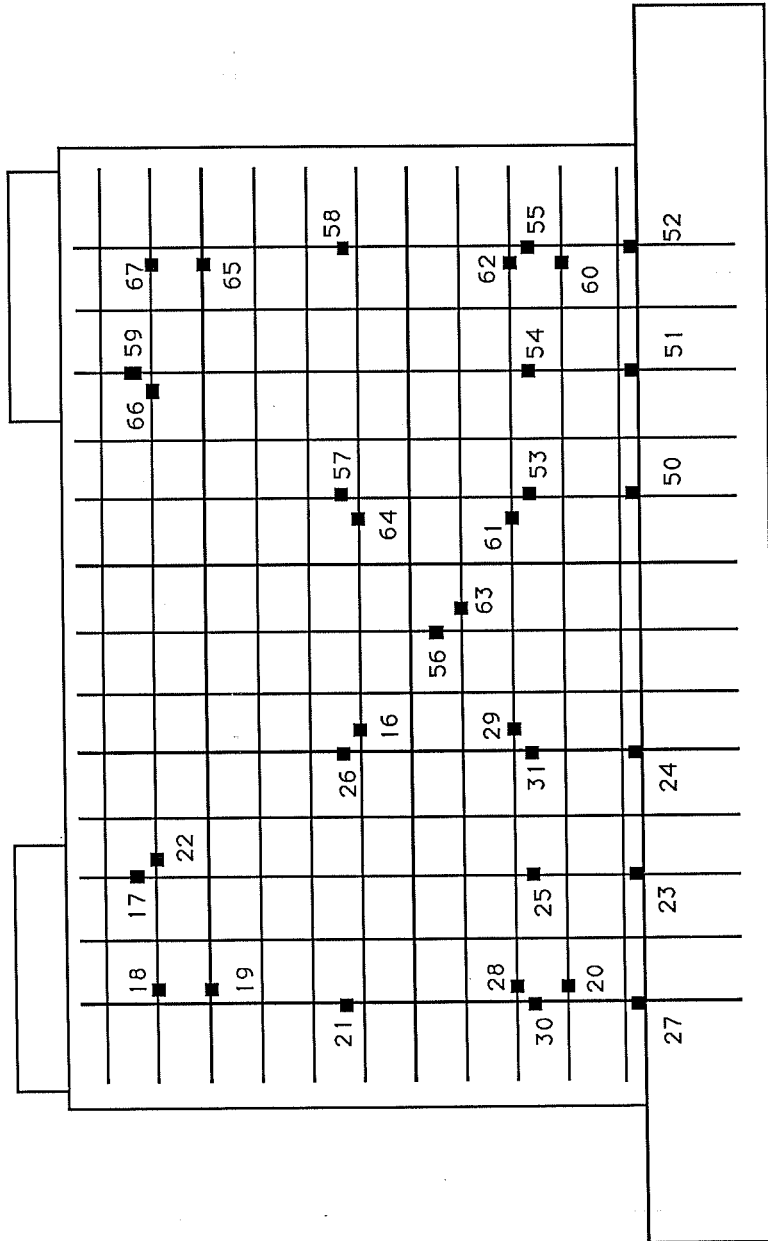


Figure 2.18a Strain Gages Locations

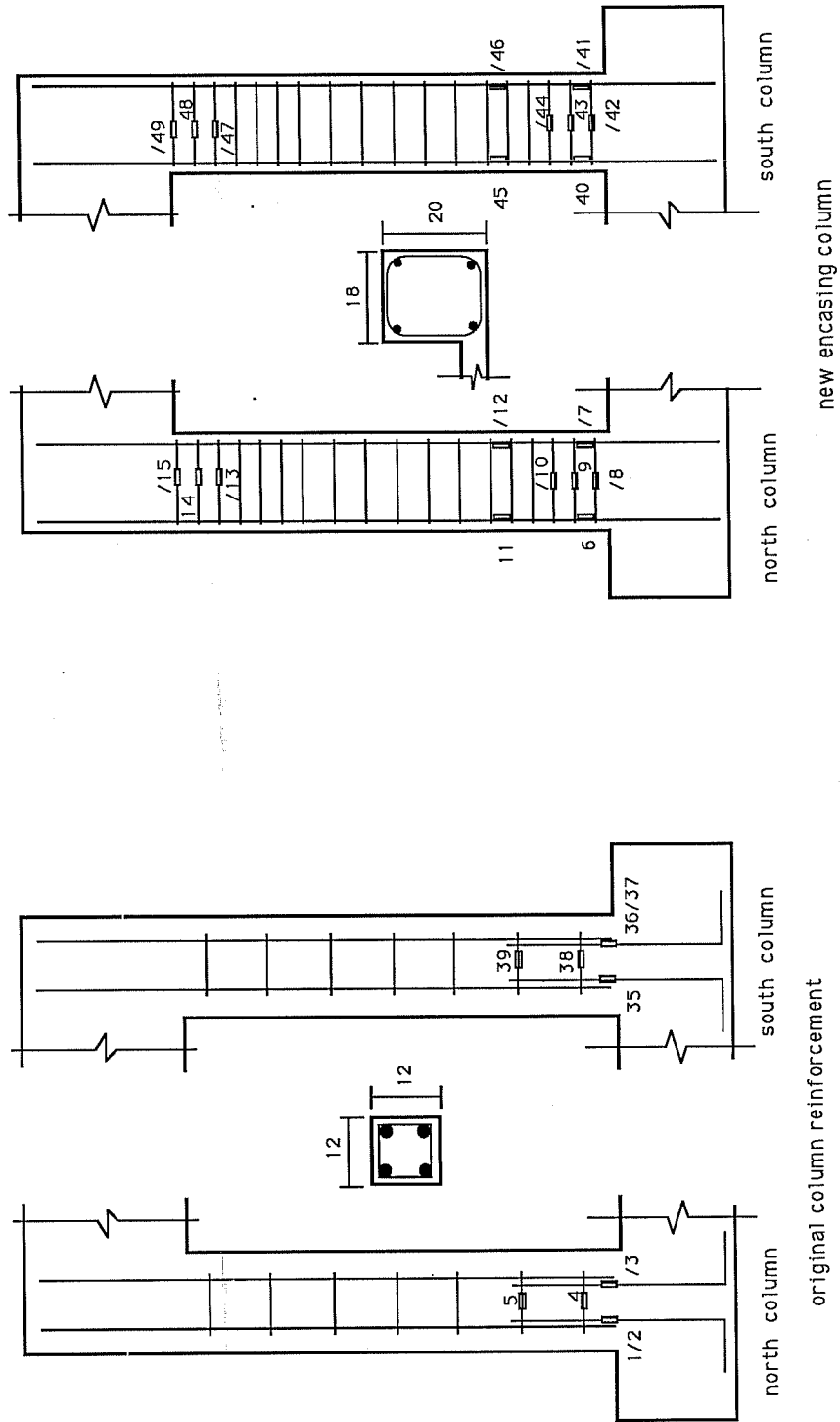


Figure 2.18b Strain Gages Locations

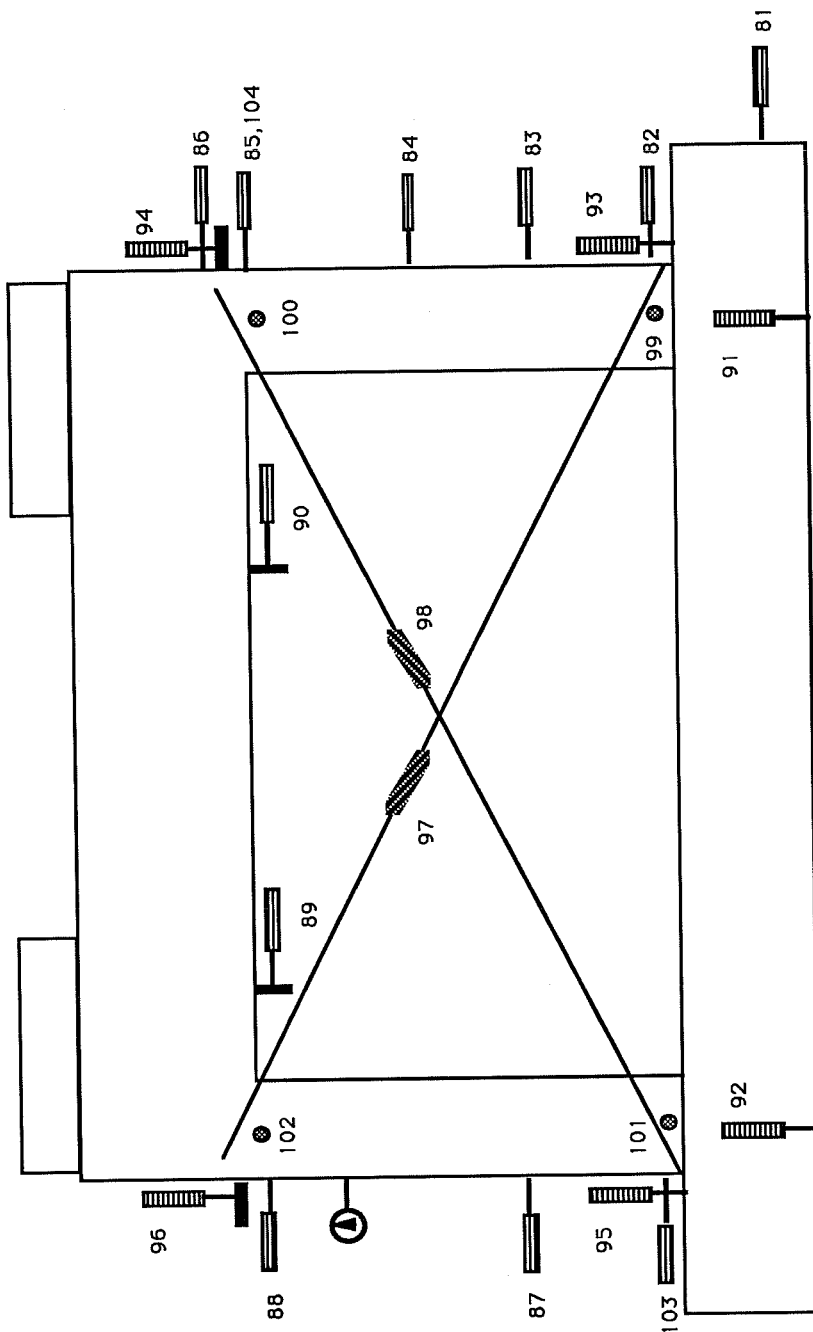


Figure 2.19 Deflection Transducer Locations

CHAPTER 3

EXPERIMENTAL RESULTS

3.1 General

The specimen was subjected to thirteen and one half load cycles. The history was load controlled up to the sixth cycle, and drift controlled from the seventh to the end of the test. The load history was chosen to permit as direct a comparison as possible between the full infill tested by Gaynor[1] and the eccentric wall test. Figures 3.1 and 3.2 show the load and drift test history. Drift is defined as the lateral displacement measured at a level at the bottom of the top beam, divided by the height of the wall. Net drift refers to that using a lateral displacement corrected to eliminate the contribution of the rigid body rotation of the specimen due to the elongation of the tiedown rods, and any lateral sliding of the foundation girder.

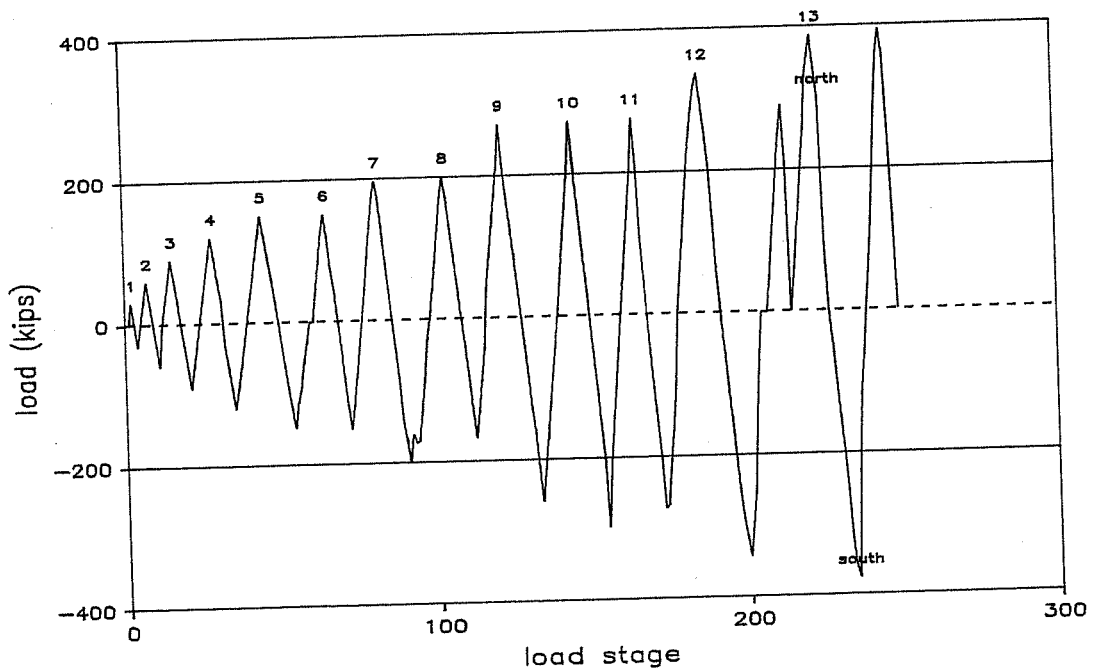


Figure 3.1 Load History

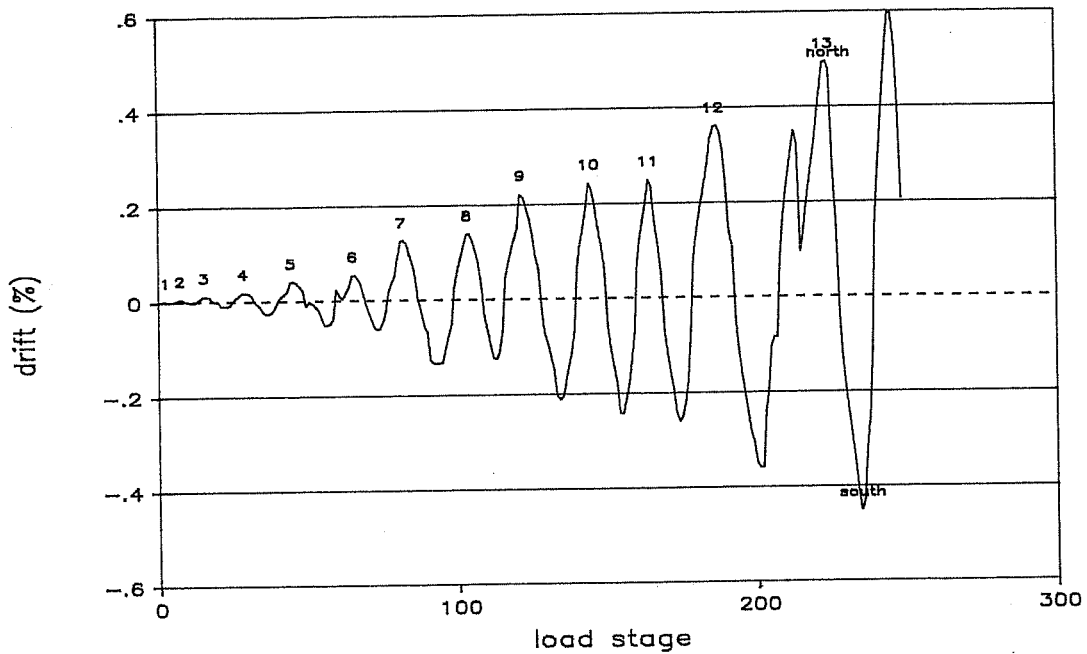


Figure 3.2 Drift History

It was observed in previous tests, [1] and [2], that the way in which load was applied and the way inclined cracks opened throughout the specimen, resulted in different measured deflections at the north and south boundary members under the same load. It was thought that a symmetric load history could be obtained only if the drift was controlled with two linear potentiometers, one located at the north face to measure the north loading drift, and one at the south face for the south loading drift measurement. The load-deflection history curve shown in Figure 3.3 is the result of the combination of the data from channels 88 and 85 (see Figure 2.8). The positive part of the hysteresis curve was obtained from channel 88 (loading north), and the negative from channel 85 (loading south).

3.2 Response to Cyclic Loading

The specimen showed fairly symmetric response in both directions. Negligible degradation of stiffness and strength was observed when repetitive cycles of equal drift were applied.

The response of the specimen was analyzed considering the crack pattern development, stiffness degradation, energy dissipation capacity per cycle, and strain progression, at different stages of the test. Measured secant stiffness is defined as the peak load in the cycle divided by the sum of the net lateral displacement and the residual displacement in the previous cycle. Figure 3.4 illustrates the secant stiffness degradation at given levels of drift normalized to the theoretical elastic stiffness. Figure 3.5 shows the energy dissipated in each cycle (area under load-displacement curve) for a given drift level (this will be discussed further in Chapter 4).

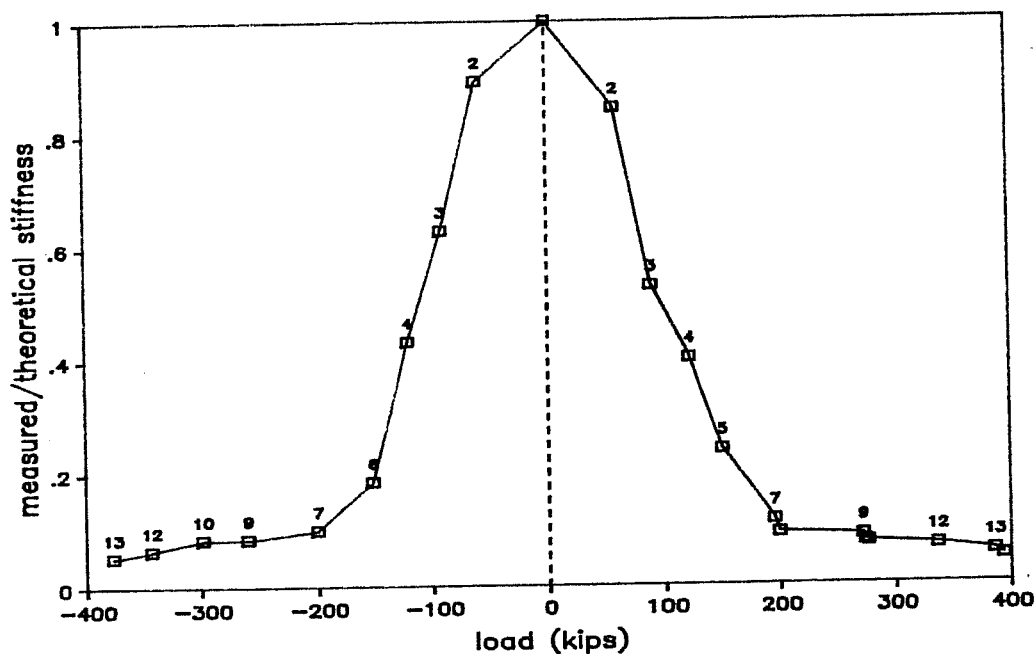


Figure 3.4 Ratio of Measured Secant Stiffness to Theoretical Elastic Stiffness

3.2.1 Cycles to 150 Kips. The specimen was subjected to single cycles to 30, 60 and 90 kips and showed an elastic response at these levels of load. The main purpose of the initial cycles was to check the instrumentation and loading set up.

The first flexural cracks appeared when the specimen was loaded north 120 kips. The cracks were located on the east face of the south column and were evenly distributed to the level of the top beam. Within three feet above the base, the cracks started horizontally but propagated as inclined torsional cracks. Inclined

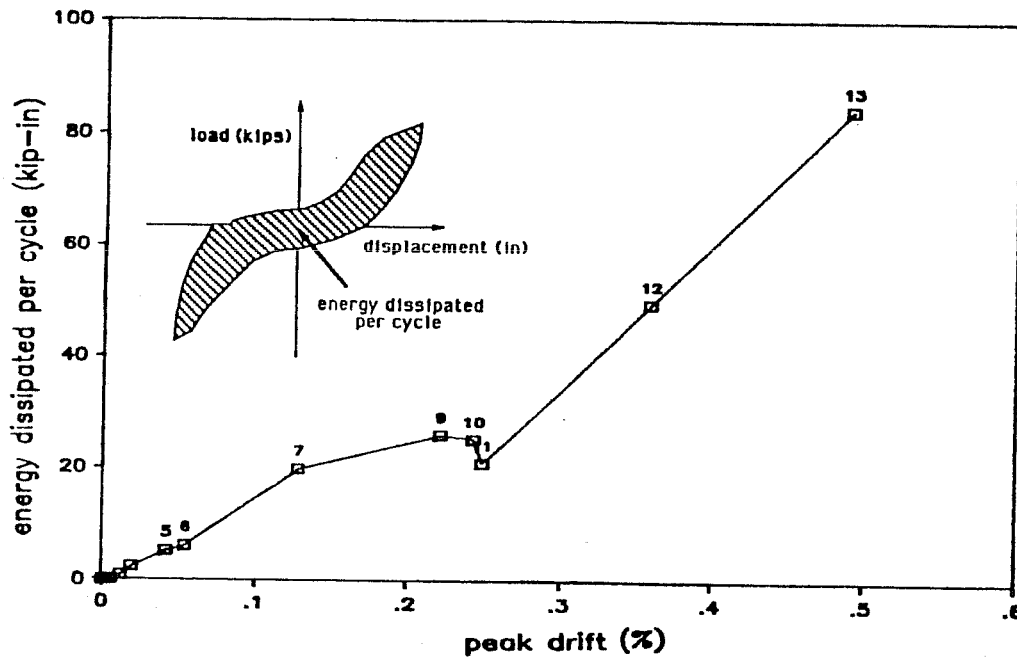


Figure 3.5 Energy Dissipated in each Cycle at Increasing Drift Levels.

cracks first appeared under loading south to 120 kips and were located at the upper south corner, with an inclination close to 45 degrees.

After two cycles to 150 kips, more inclined cracks formed in the download corner, as shown in Figures 3.6 and 3.7. Flexural cracks propagated up to two feet into the wall. Measured secant stiffness, Figure 3.4, was about 20% of the theoretical elastic stiffness for this direction of loading. The energy dissipated per cycle at this stage was negligible.

3.2.2 Cycles to 0.1% Drift [Cycles 7 and 8]. Beyond the cycles to 150 kips, the load history was drift controlled. The specimen was subjected to two cycles at 0.1% drift and reached an average peak load of 200 kips.

During the first cycle, more inclined shear cracks formed throughout the wall as shown in Figures 3.8 and 3.9. A better distribution of inclined cracks was observed when loading south, but more flexural cracks were found in the south column when loading north. Neither the inclined cracks nor the flexural cracks propagated into the top beam. Vertical cracks formed at the very top of the wall, extending three feet down into the wall and appeared to be a result of the concentrated stresses in

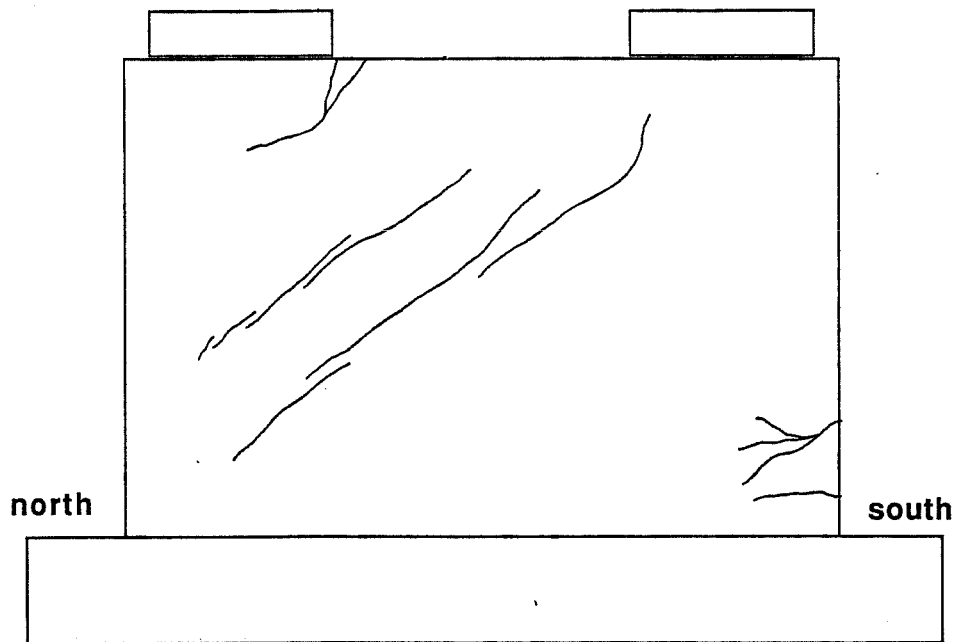


Figure 3.6 Crack Pattern at 150 kips (Loading North)

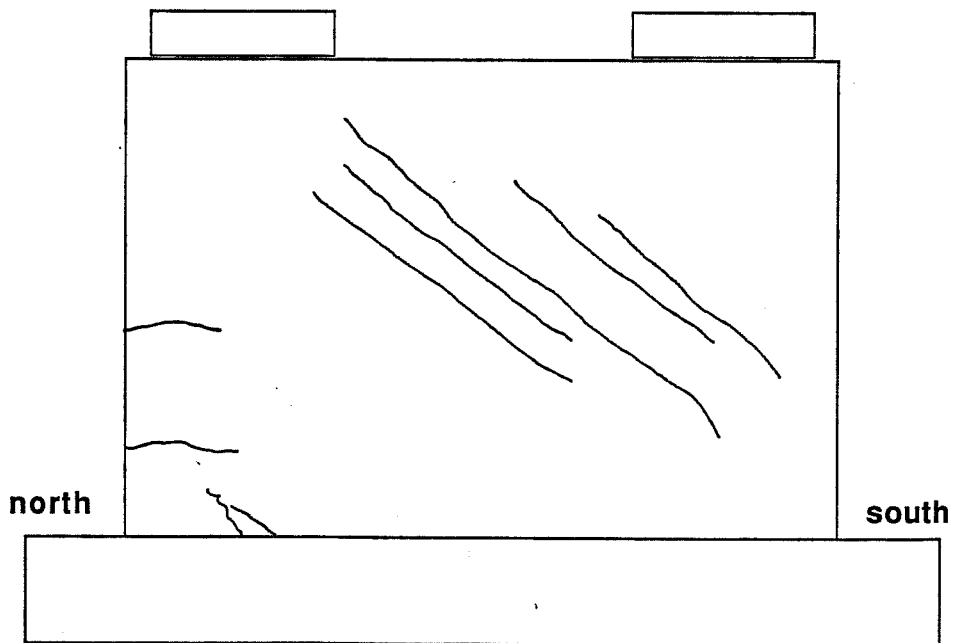


Figure 3.7 Crack Pattern at 150 kips (Loading South)

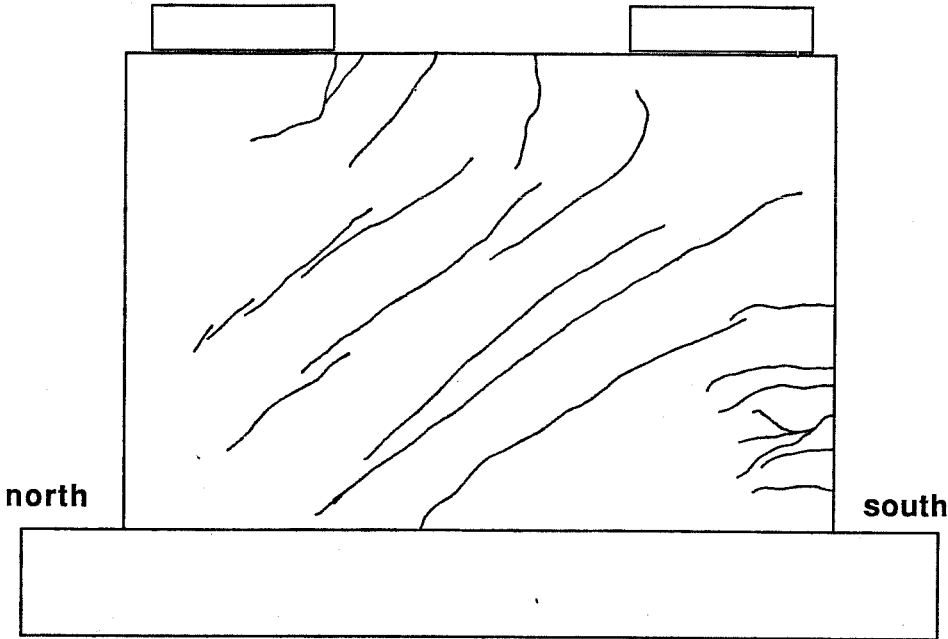


Figure 3.8 Crack Pattern at 0.1% Drift (Loading North)

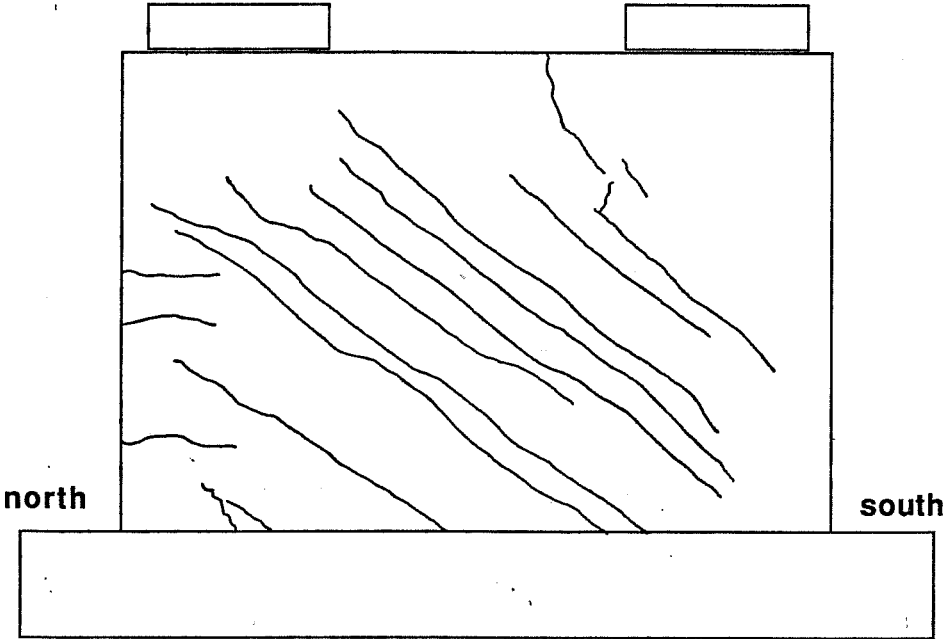


Figure 3.9 Crack Pattern at 0.1% Drift (Loading South)

the loading blocks. During the second cycle, no change in the crack pattern was observed.

The secant stiffness dropped to 11% of the theoretical value in the first cycle to 0.1% drift, and to 9% during the second cycle. The pronounced change in stiffness was associated with the widening of shear cracks in these cycles.

Yielding of the flexural reinforcement was observed first in one of the bars forming the jacket around the north column, during loading to the south. The rest of the steel in the north column was about 50% of yield strain. Strains at the base of the south column (loading north) reached 75% of yield.

The normalized energy dissipated per cycle (Figure 3.5) started to be significant, it was 95 kips.

3.2.3 Cycle to 0.2% Drift [Cycles 9,10 and 11]. Three reversed cycles to 0.2% drift were applied. The peak load for the north and south loading were remarkably steady and symmetric, with an average value of 275 kips.

During the first cycle, new inclined cracks formed with an approximate angle of 35 degrees. The amount of cracking was greater when loading north, so that the asymmetric pattern developed in the previous cycles, became similar for both direction of load. Main inclined cracks opened to 0.03 in. during the peak load. Extensive flexural cracking formed in the north column (loading south), and was well distributed throughout the height of the column. Some of the horizontal column cracks turned into inclined shear cracks as they propagated into the wall. Crack patterns at this stage are illustrated in Figures 3.10 and 3.11. No additional cracks formed during the second and third cycles to 0.2% drift.

The secant stiffness (Figure 3.4) in the first cycle to 0.2% drift was 8% of the theoretical value, did not change in the second cycle, and dropped to 7% in the third cycle. The normalized energy dissipated per cycle was 30% greater in the first cycle than in the third cycle (Figure 3.5) due to the pinching of the hysteresis loops.

A strain profile along the base of the wall, Figures 3.12 and 3.13, show that when the load was applied north, the vertical steel within 10 ft. of the south column reached 75 to 85% of yield. On the other hand, when loading south, the

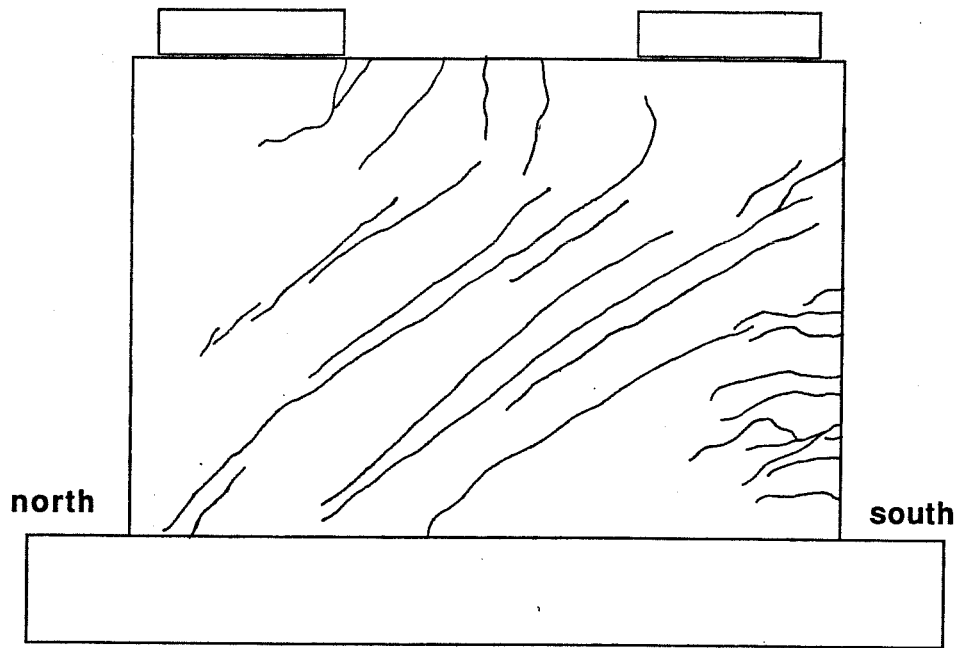


Figure 3.10 Crack Pattern at 0.2% Drift (Loading North)

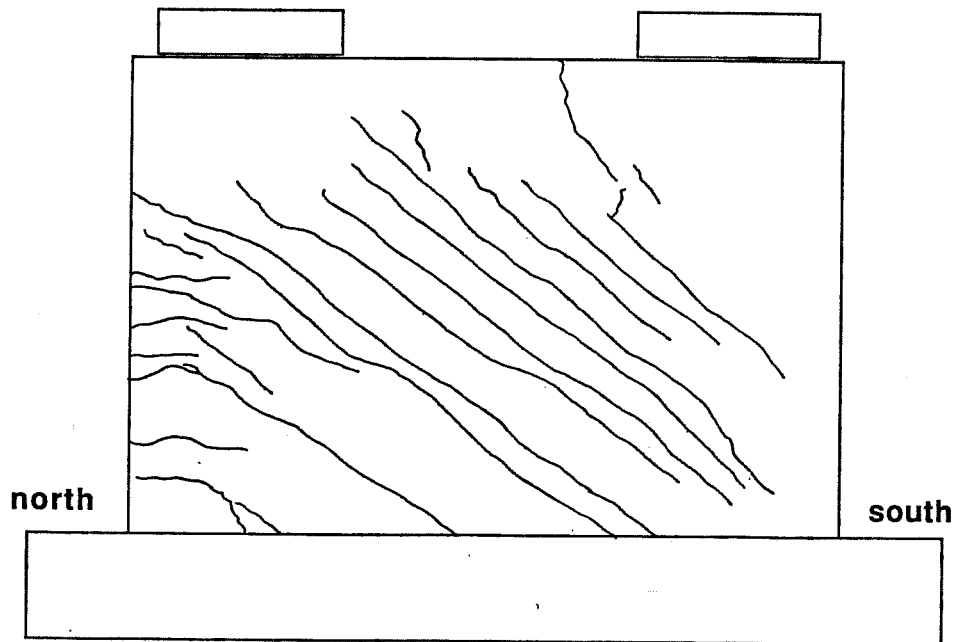


Figure 3.11 Crack Pattern at 0.2% Drift (Loading South)

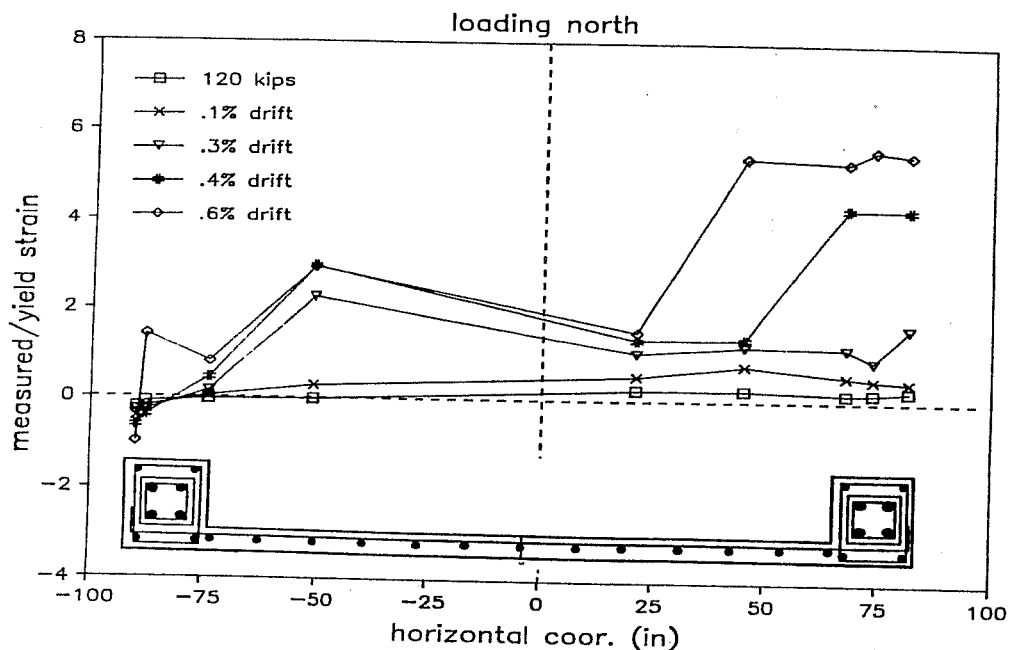


Figure 3.12 Steel-Strain Profile at the Base of the Wall (loading North)

vertical steel within 4 ft. of the north column face exceeded yield, but the steel in the original column reached only 80% of the yield.

3.2.4 Cycle to 0.3% Drift [Cycle 12]. A single cycle to 0.3% drift reached an average peak load of 340 kips. No new cracks were found in the specimen but cracks extended toward the base and the top of the wall. As shown in Figures 3.14 and 3.15, inclined cracks were spread throughout the wall but not in the flexural compression zone. Well defined concrete struts were formed at inclinations of 35 to 45°. Major inclined cracks opened to 0.05 in. during the peak load.

As the crack pattern did not change with the drift increment, the secant stiffness remained the same at 6.5% of the theoretical value. Normalized energy absorption capacity was 65% greater than that in the last 0.2% drift cycle.

Strain profile along the base of the wall, Figures 3.12 and 3.13, indicated that all the flexural steel in the column and the wall within 12 ft. of the upload face was above yield. Longitudinal reinforcement in the jacket reached strains up to five times yield while the existing column reinforcement reached a value of about twice yield.

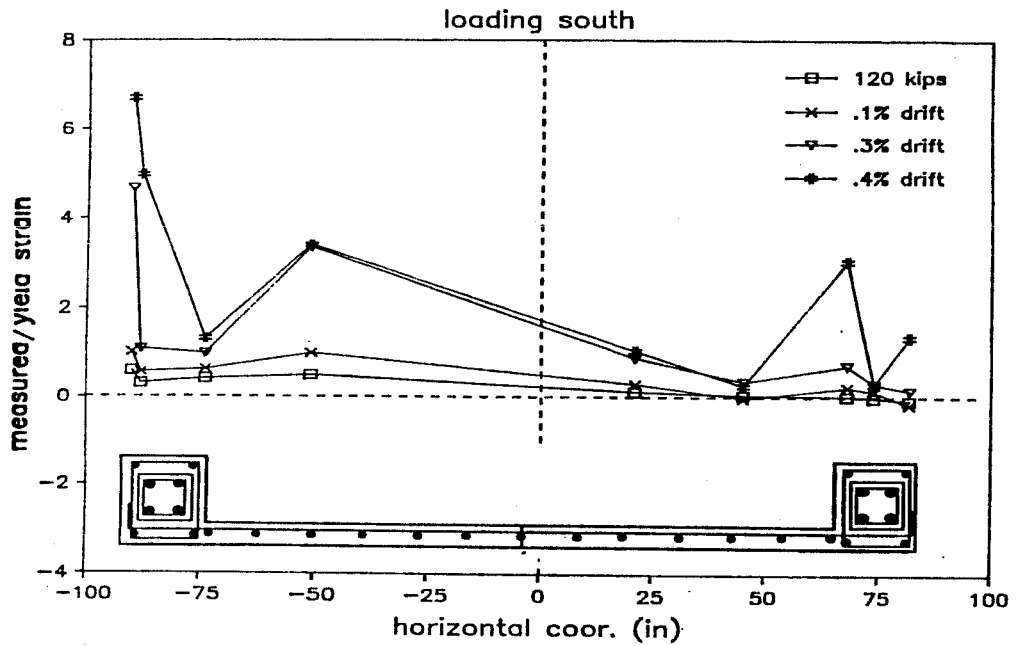


Figure 3.13 Steel-Strain Profile at the Base of the Wall (Loading South)

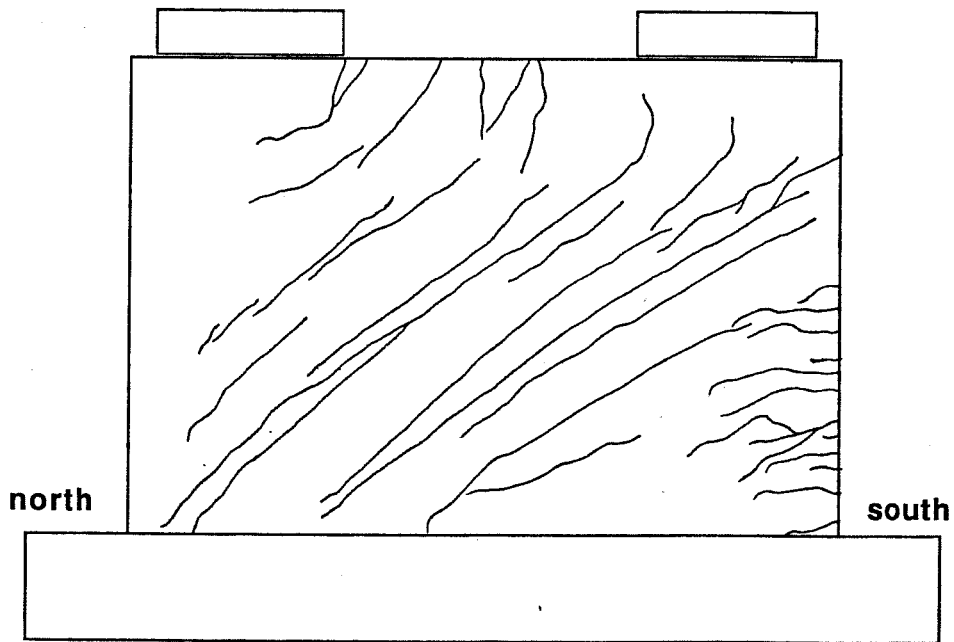


Figure 3.14 Crack Pattern at 0.3% Drift (Loading North)

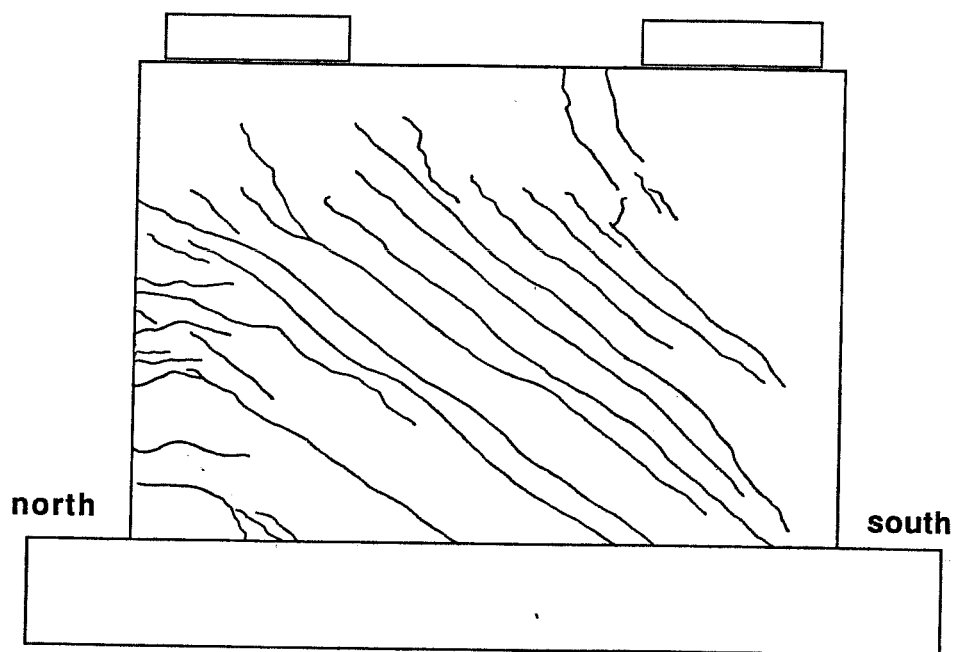


Figure 3.15 Crack Pattern at 0.3% Drift (Loading South)

3.2.5 *Cycle to 0.4% Drift [Cycle 13]*. The average peak load in this cycle was 380 kips. Changes in the crack pattern were limited to extension of some of the inclined cracks toward the base and the top of the wall when it was loaded north. No additional flexural cracks formed from this point until the end of the test. Major inclined cracks opened to 0.08 in.. After this cycle the crack pattern was remarkably symmetric in both directions of loading as illustrated in Figures 3.16 and 3.17.

The secant stiffness was about the same in both directions of loading, 6% of the theoretical value. A major change was observed in the normalized energy dissipated during this cycle, with most of the flexural reinforcement yielding, it increased to 120 kips, 30% greater than the previous cycle to 0.3% drift. Strain profiles along the base of the wall, Figures 3.12 and 3.13, show that with the exception of the steel in the compression zone, strains in the vertical steel were beyond yield, up to seven times yield in the encasing reinforcement, and up to five times in the existing frame reinforcement. Another profile of strains 21 in. above the base of the wall, which is just at the end of the column splice, showed the vertical reinforcement exceeded yield within 11 ft. from the upload face of the specimen. Gages placed

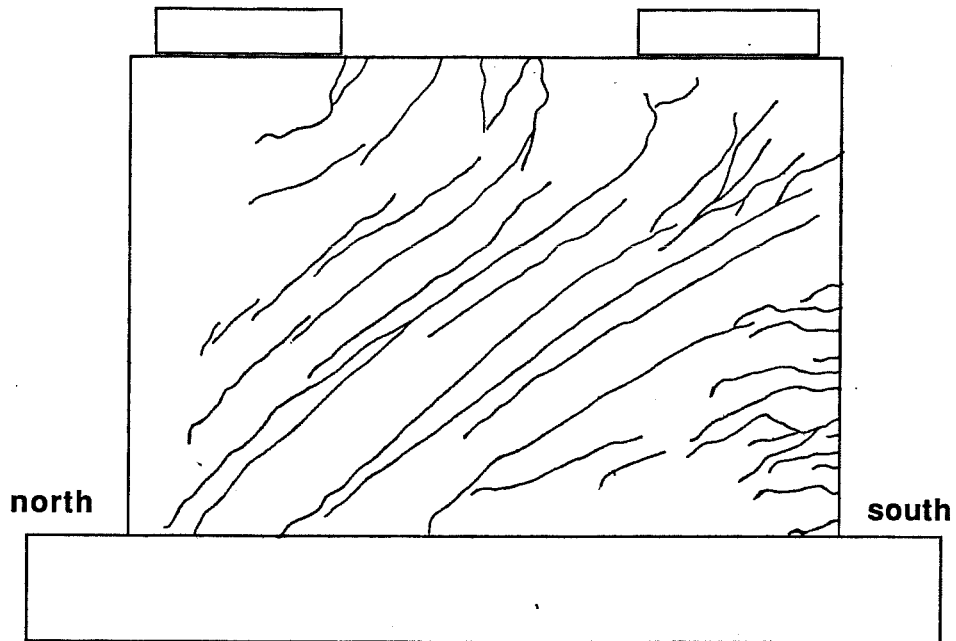


Figure 3.16 Crack Pattern at 0.4% Drift (Loading North)

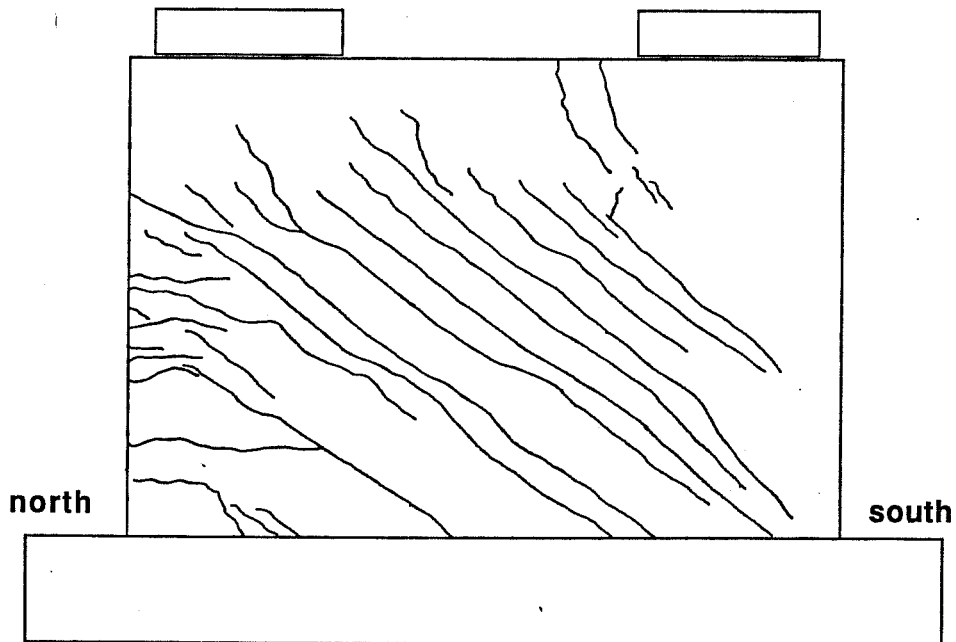


Figure 3.17 Crack Pattern at 0.4% Drift (Loading South)

at the midheight of the wall, 5 ft. above the base, indicated values over yield in a region around the upload boundary members.

3.2.6 Cycle to 0.6% Drift [Cycle 14]. The specimen was subjected to one half cycle to 0.6% drift, loading north, reaching a peak load of 410 kips according to the X-Y plotter. The peak reading taken by the computer registered 394 kips after some pressure loss in the hydraulic line. High pressure in the lines, over the 10 ksi design value, made the rams and hoses leak, and did not allow continuation of the test.

The crack pattern did not change. Figure 3.18 shows the final distribution of cracks. Secant stiffness dropped to 4.5% of the theoretical value. The gain in strength with the increment of drift was small, suggesting that the specimen reached peak strength.

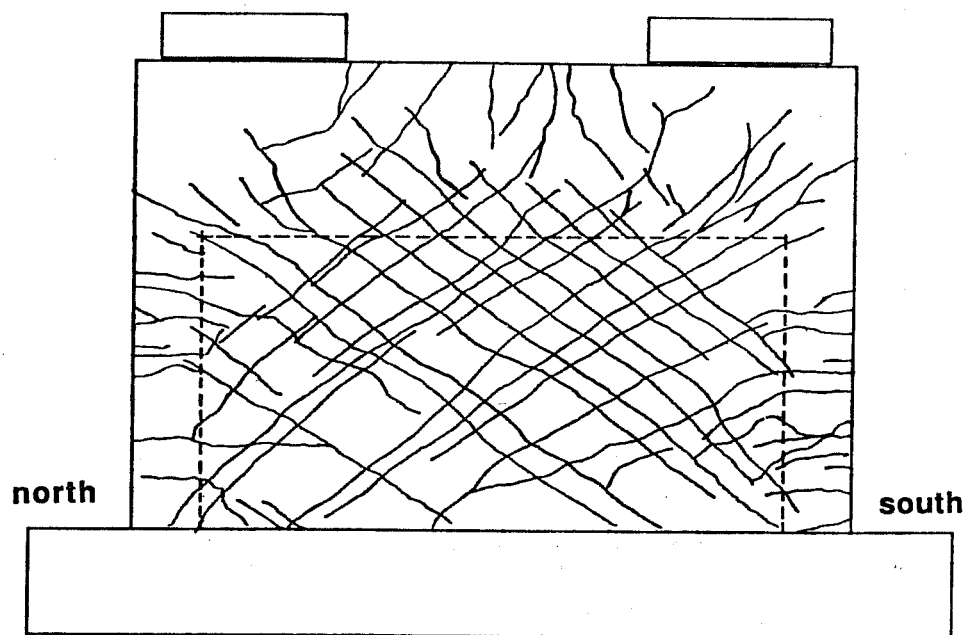


Figure 3.18 Crack Pattern After Completion of the Test

Measured strains at the base of the wall, Figure 3.12, reached up to nine times yield in the encasing reinforcement, and six times yield in the existing column reinforcement.

3.3 Column Splice

The splice at the base of existing columns, originally designed for compression load, showed excellent behavior under cyclic loading. Strain increases monitored at the base of columns showed up to 6.5 times yield in the south column (loading north), and up to 5 times yield in the north column (loading south). Figures 3.19 and 3.20 illustrate typical behavior of the flexural reinforcement in the boundary members. The load-strain curve shows the ability of the specimen to develop the ductility demanded. The absence of vertical cracks in the splice region and the continuous increase in strain with load indicated the success in avoiding failure of the splice in tension. Higher strains were observed in the encasing reinforcement than in the existing column reinforcement, suggesting that some slip occurred through the interface of the old and new concrete.

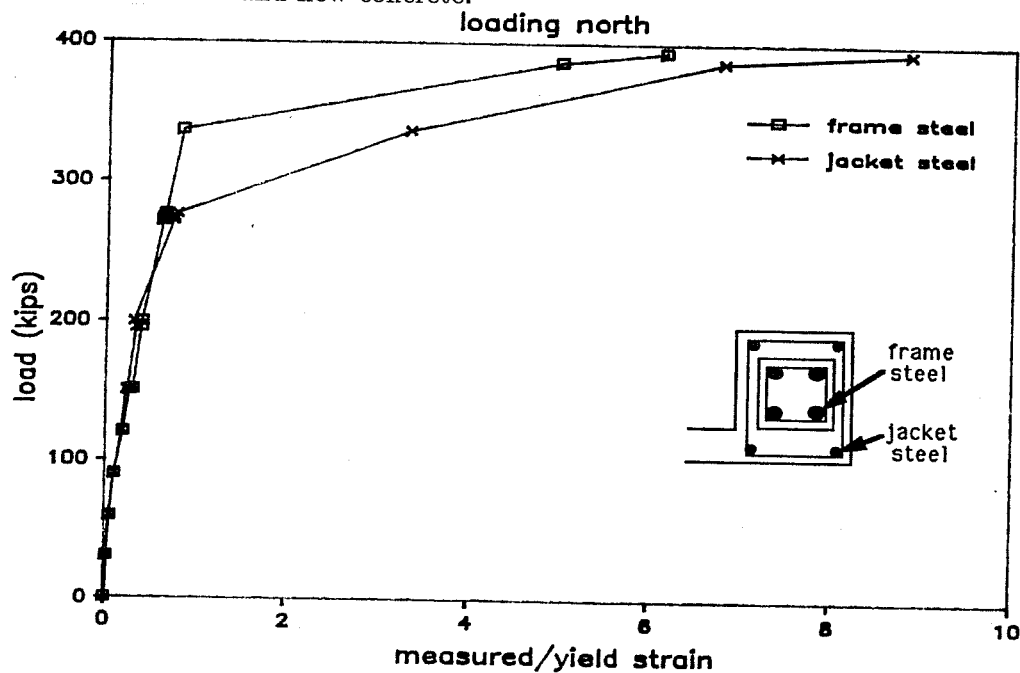


Figure 3.19 Load-Strain Relationship Longitudinal Reinforcement in South Boundary Member

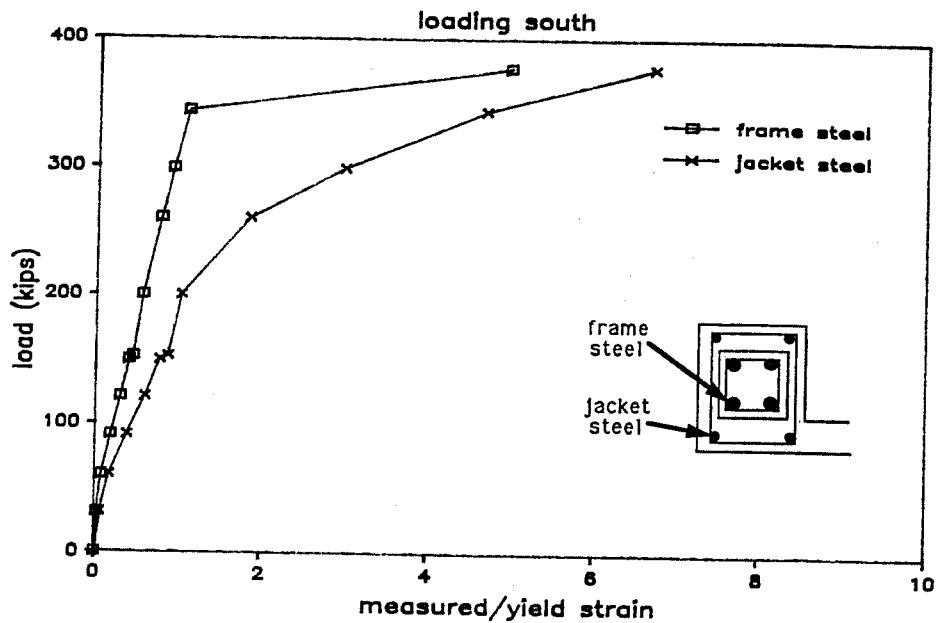


Figure 3.20 Load Strain Relationship Longitudinal Reinforcement in North Boundary Member

3.4 Shear Connector Dowels

Six of the fifteen dowels epoxy grouted in the top beam (shown in Figure 2.5) were monitored to obtain the strains throughout the test (See Figure 2.18). Although they were designed to transfer the entire shear from the existing frame to the wall, they did not develop the strains expected, only 10% of yield was reached at the most strained dowel. This leads to the conclusion that most of the shear was transferred not by the dowels but through the encasing element, concrete and stirrups through the plane of failure, a mechanism stiffer than the dowels'. Figures 3.21 and 3.22 illustrate typical load-strain curves of the epoxy grouted dowels for both loading directions.

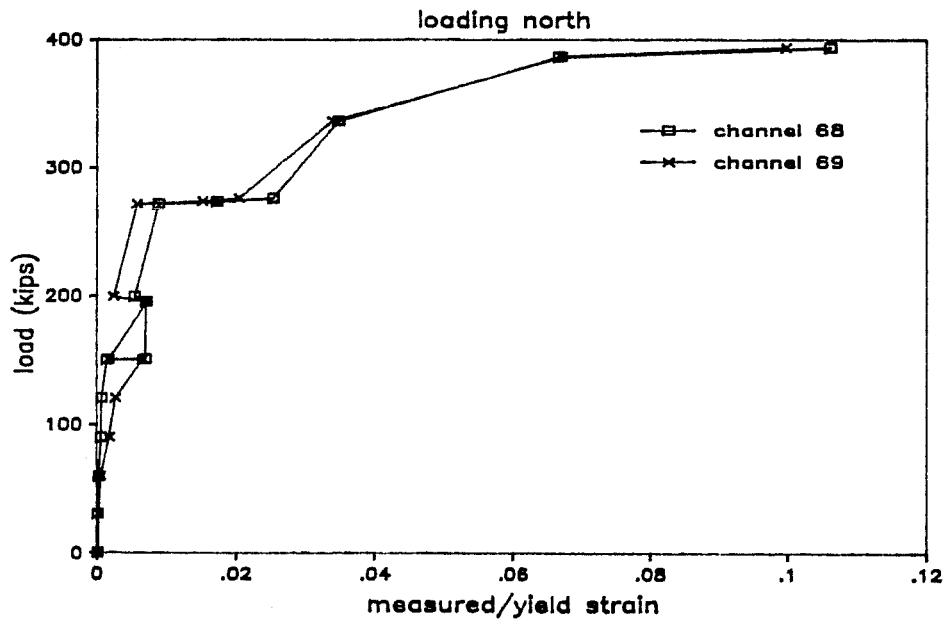


Figure 3.21 Load-Strain Relationship for Dowel Connectors (Loading North)

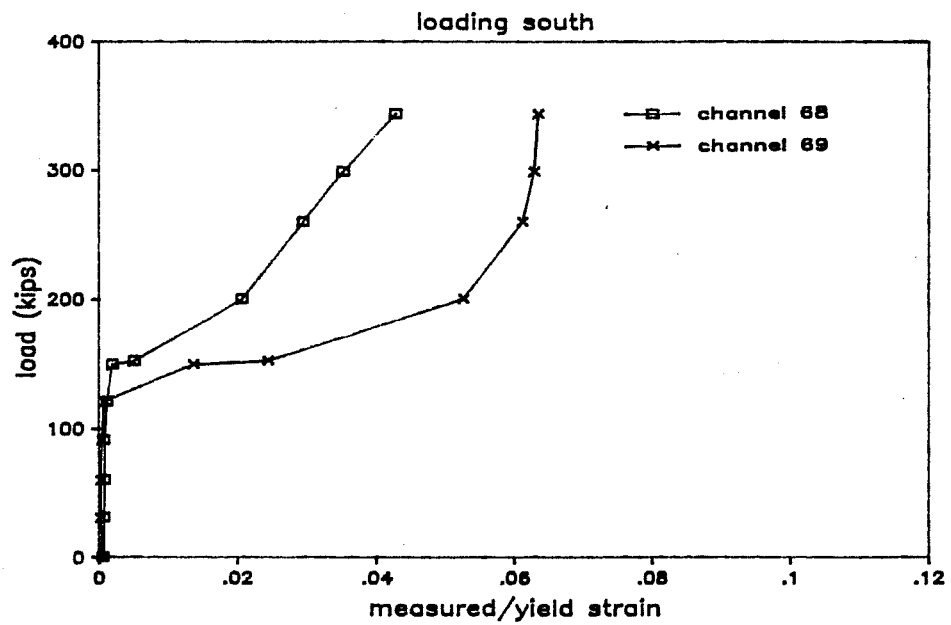


Figure 3.22 Load-Strain Relationship for Dowel Connectors (Loading South)

CHAPTER 4

EVALUATION OF EXPERIMENTAL RESULTS

4.1 Lateral Displacement Response

The displacement response to lateral loads in a structure is commonly referred to as the lateral stiffness. Lateral stiffness can be calculated using classical mechanics of materials theory based on a linear elastic response. But for reinforced concrete structures the stiffness suggested by most codes accounts for only a fraction of the total because of the loss of stiffness due to cracking and cyclic load degradation. In the following sections, a comparison between the theoretical and measured stiffness provide a means for determining the expected response of similar substructures for design purpose.

4.1.2 Theoretical Lateral Stiffness. The elastic response of a reinforced concrete wall to lateral loads can be predicted using classical mechanics of materials. Modeling the test wall as a cantilever beam, the shear and flexural deformations were obtained assuming linear elastic behavior. The following assumptions were made:

- a) The modulus of elasticity of the concrete is

$$E = 57000 \sqrt{f'_c}$$

- b) Shear modulus of the concrete is

$$G = \frac{E}{2(1 + \nu)}$$

- c) The section is uncracked.
- d) Plane sections remain plane.
- e) Concrete properties are the same in the existing frame and strengthening elements. The specimen has monolithic behavior, even though the wall is added to an existing frame.
- f) No contribution of the reinforcement

The lateral displacement u at the bottom of the top beam due to a lateral load applied at the top of the wall is given by the formula:

$$u = \frac{Ph_1}{3EI_1} + \frac{Ph_1}{A_1G} + \frac{Ph_1^2h_2^2}{2EI_1} \quad (1)$$

where the first term of equation (1) is the lateral deflection due to flexure over the height of the wall h_1 . The second term is the displacement due to shear deformation, and the third term is the lateral displacement due to the moment created at the bottom of the top beam by the lateral force acting through the height h_2 . Figure 4.1 shows the terminology used in equation (1).

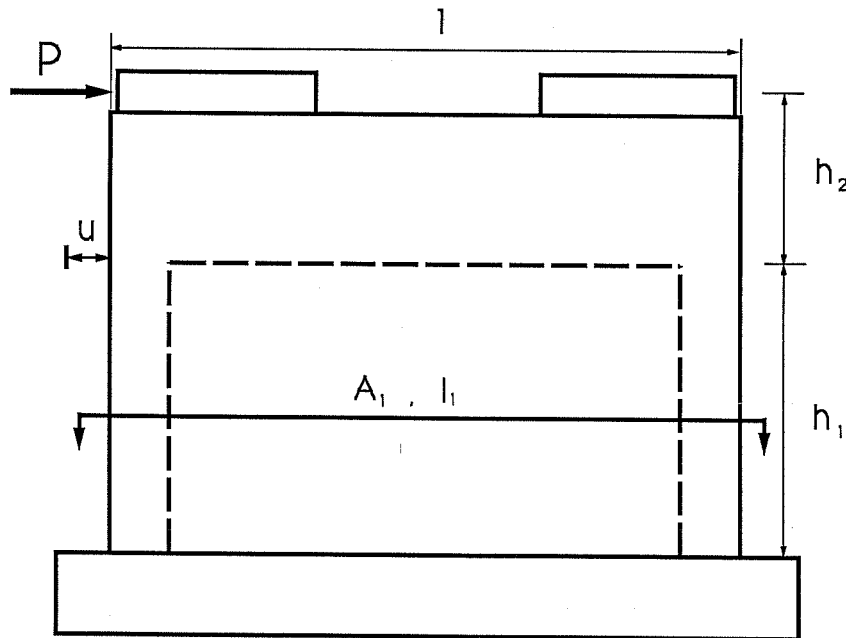


Figure 4.1 Theoretical Stiffness Variables

Substituting values from the test specimen into equation (1) leads to a lateral stiffness equal to 14,300 kip/in. Shear displacement accounts for 78% of the total stiffness and 22% is due to bending effects.

4.2.3 Measured Lateral Stiffness. Measured stiffness refers to the secant stiffness defined as the peak load in a cycle divided by its associated lateral displacement. The measured initial elastic stiffness was not considered a reliable value

because the lateral displacements at these stages of load were below the sensitivity of the instruments. Figure 4.2 shows the load versus the ratio of measured to theoretical stiffness. From the beginning of the test to cycle 7 (200 kips, 0.1% drift) the stiffness sharply declined from 100% to 11% of the theoretical value. Measured stiffness at first cracking (cycle 4, 120 kips, 0.02% drift) was 45% of the theoretical value. From cycle 7 to the end of the test, the degradation gradually declined from 11% to 5% of the theoretical stiffness.

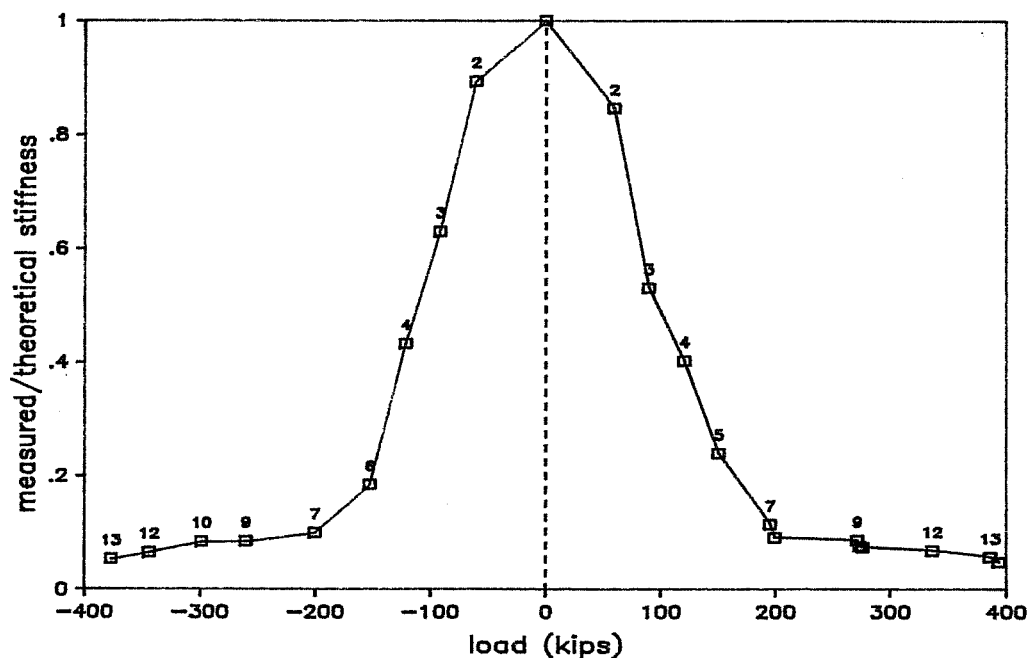


Figure 4.2 Ratio of Measured to Theoretical Stiffness vs. Load

4.2 Deflection Components

Lateral deflection was divided into three components; shear deformation, flexure, and fixed end rotation (lack of fixity at the base of the wall). The deflection components provide a means of determining the predominant mechanism influencing the response at different stages of the test.

Measured deflection components were obtained from linear potentiometers shown in Figure 4.3. Displacements smaller than 0.01 in. were not considered reliable due to the sensitivity of the instruments. The fixed end rotation component (u_f),

was obtained using the rigid body model shown in Figure 4.4. Neutral axis locations were assumed to be at the geometric centroid of the section up to first cracking, and at the interior face of the boundary element (18 in. compression depth) after first cracking. The error induced by assuming constant compression depth after first cracking was negligible.

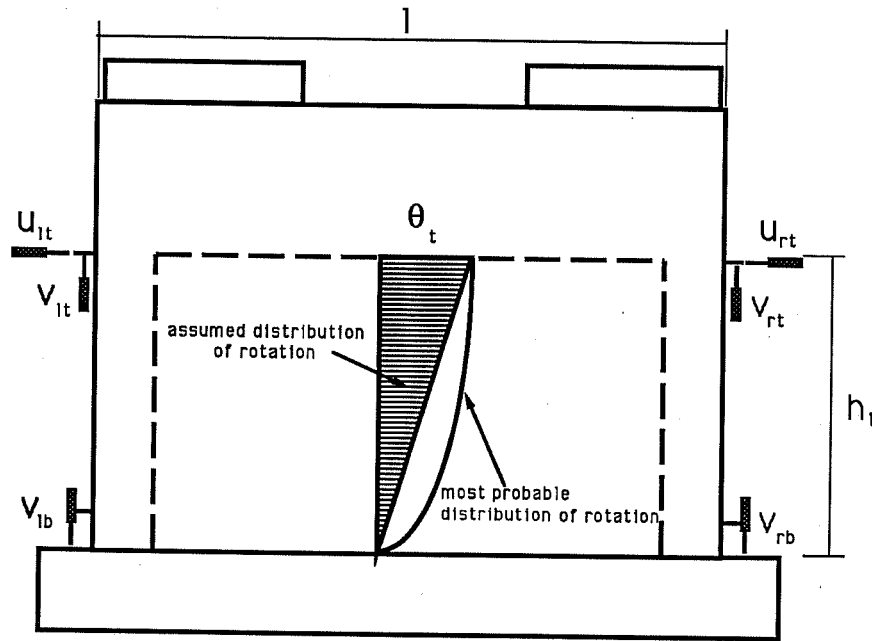


Figure 4.3 Instrumentation for Determining Deflection Components

The flexural component of deformation was obtained assuming a linear distribution of rotation, from zero at the base of the wall to Θ_h at the bottom of the top beam. According to the terminology shown in Figure 4.3, the flexural component is given by

$$u_b = \int_0^h \Theta_y d_y \quad (3)$$

$$\Theta_y = \frac{y}{h} \Theta_h$$

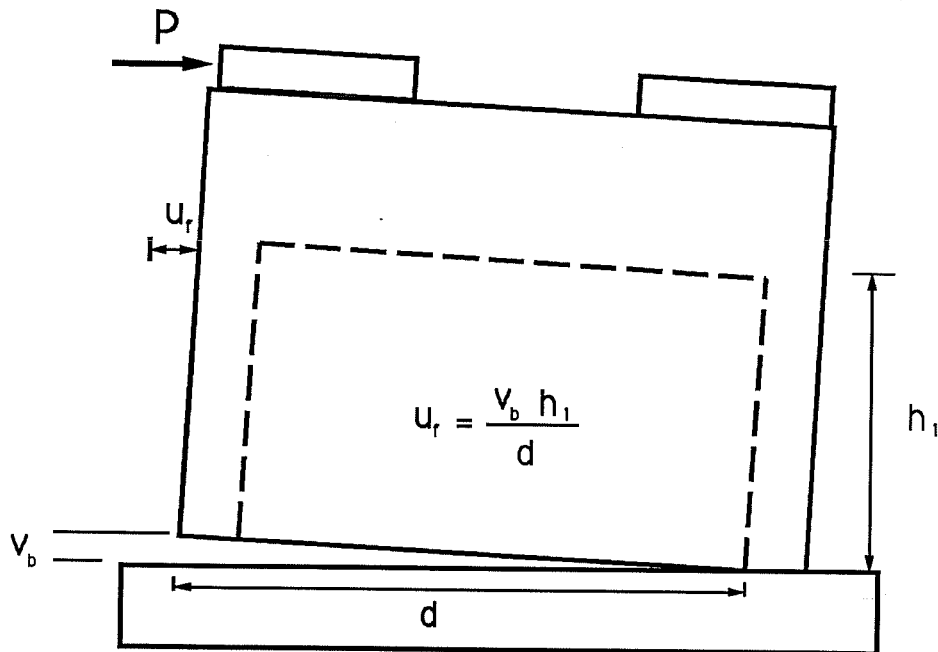


Figure 4.4 Fixed-End Rotation Effect

$$\Theta_h = \frac{(v_{lt} - v_{lb}) - (v_{rt} - v_{rb})}{l}$$

solving equation (3)

$$u_b = \frac{h \Theta_h}{2l}$$

The assumption of a linear distribution of rotation over the height results in underestimation of the flexural component and an overestimation of the shear contribution. In future tests, the estimation of the rotation distribution would be improved by measuring the rotation at midheight or at other intermediate heights using a piecewise linear distribution of rotation.

The shear deformation component was the difference between the total lateral displacement and the sum of the components due to fixed-end rotation and flexure.

$$u_s = \frac{(u_{lt} - u_{rt})}{2} - u_b - u_f \quad (5)$$

Figure 4.5 shows the displacement components versus load, and Figure 4.6 shows the contribution of each deflection component normalized to the total deflection. Before cracking of the wall above the base, 31% of the lateral deflection was due to the fixed-end rotation. The flexural component accounted for 8% of the total, and the shear component about 60% of the total. After the wall reached cracking, the flexural component reached its maximum when the flexural steel started to yield. At this point, 17% of the total displacement was due to bending and 73% due to shear deformation.

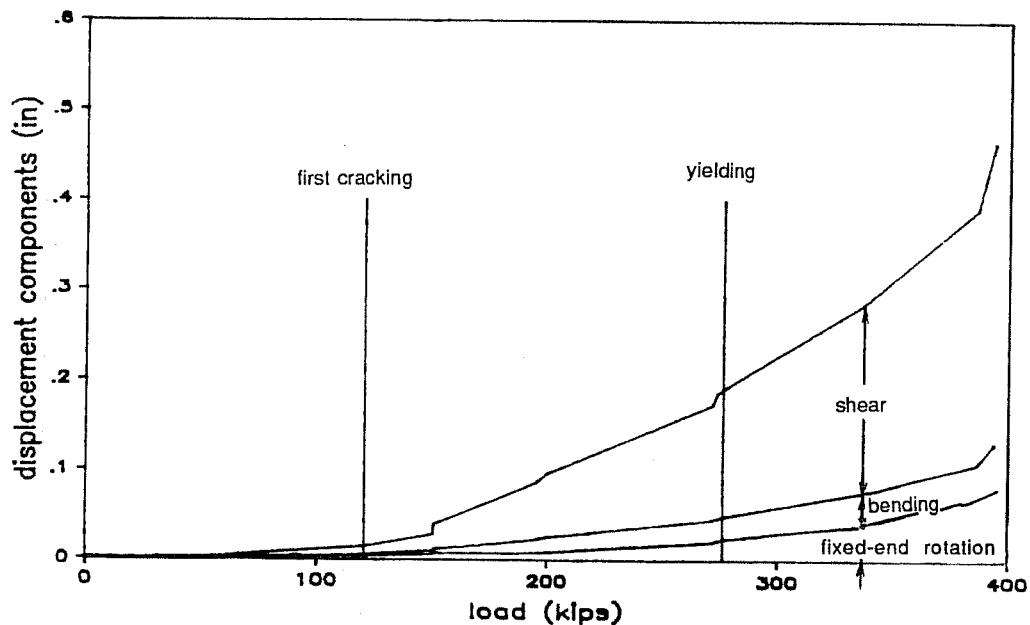


Figure 4.5 Lateral Deflection Components

From yield to the end of the test, the flexural component gradually decreased from 17 to 11%. The fixed-end rotation component increased from 10% at first yield to 17% at the end of the test. Although many cracks developed after first yield, the shear component remained constant (about 72% of the total displacement).

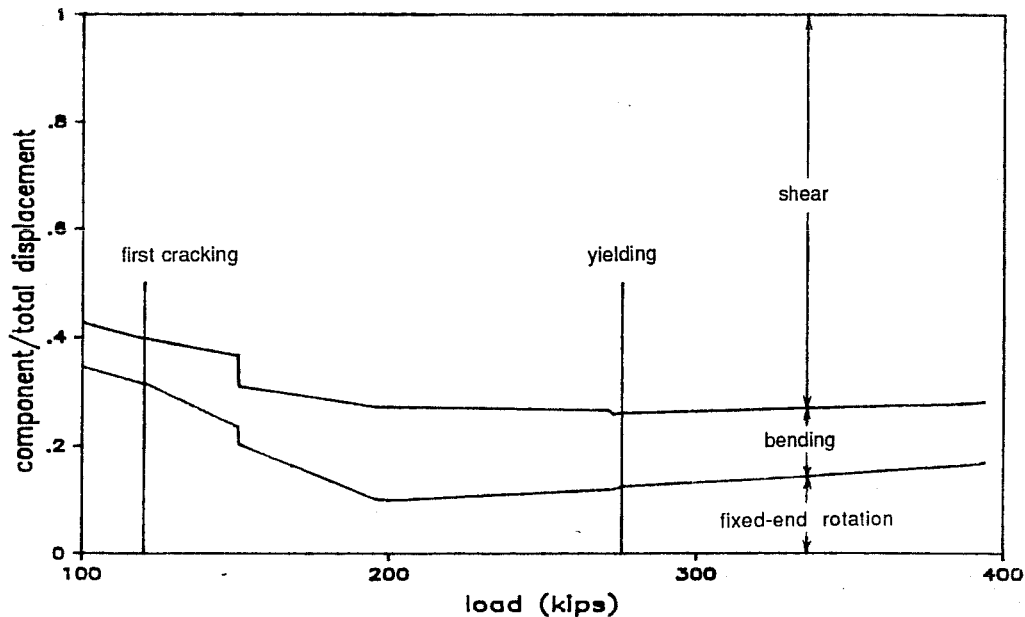


Figure 4.6 Deflection Component Ratios

4.3 Prediction of Strength

Flexural and shear strength were predicted by common methods used in structural design. Unless specified otherwise, the following assumptions were used in analysis.

- a) Design methods used for monolithic reinforced concrete are valid for the specimen.
- b) Torsional moment induced by the eccentricity of the load does not influence the in-plane behavior.
- c) Mechanical properties of materials are the same for the entire specimen.
- d) Concrete compression strength is 4500 psi.
- e) Steel reinforcement is Grade 60.

4.3.1 Flexural Cracking Strength. Flexural cracking strength was computed using classical mechanics of materials theory where the cracking moment is given in the ACI 381-86 code by

$$M_{cr} = \frac{f_r I_g}{Y_t} \quad (6)$$

where $f_r =$ modulus of rupture of concrete $= 7.5 \sqrt{f'_c}$

$I_g =$ moment of inertia of the gross section.

$Y_t =$ distance from the centroid to the extreme tension fiber.

Equation (6) yields

$$M_{cr} = 33,819 \text{ kip-in or } V_{cr} = 268 \text{ kips}$$

It was observed that the code overestimates the flexural cracking strength of the specimen, in which first flexural cracking above the base occurred during the 120-kip load cycle. The fact that the original columns were already cracked in the previous test [1], shrinkage, and that the concrete strength of the existing frame was lower than that of the eccentric wall are possible reasons for the difference between the code and test cracking strength.

4.3.2 Flexural Strength.

4.3.2.1 Analysis Using ACI Code Assumptions. The maximum flexural strength was calculated using the specified material properties, assuming linear variation of strain along a section, and an equivalent rectangular concrete stress block as suggested by ACI 318-86. No axial load was applied to the wall nor considered in the analysis. Assuming the compression block to lie within the boundary column (see Figure 4.7 for nomenclature), leads to a depth of the equivalent rectangular compression zone of

$$a = \frac{A_s f_y}{0.85 f'_c b} = 5.8 \text{ in.}$$

from which,

$$M_n = A_{si} f_y (d_i - a/2) = 4142 \text{ kip-in. or } V_n = 394 \text{ kips}$$

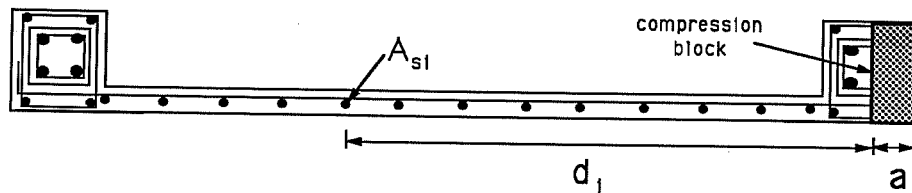


Figure 4.7 Notation for Flexural Analysis of Wall

The code analysis proved to be a conservative but realistic estimation, considering that the gain of strength was small as the drift increased near the end of the test.

4.3.2.2 Refined Analysis. The maximum flexural strength was calculated using a more refined analysis. The cross section showed in Figure 2.2 was analyzed to obtain the corresponding moment-curvature relationship. The computer program RCCOLA [5] was used, and the following assumptions were made:

- a) Plane sections remain plane.
- b) The stress-strain relationships used for the steel and concrete were the same in the entire specimen and are shown in Figures 4.8 and 4.9.
- c) No axial load was considered in the analysis.

Unconfined and confined sections were analyzed. For the confined section, the model proposed by Scott, Park and Priestley[7] was used. No significant difference was found using confined and unconfined sections. Figure 4.12 shows the moment-curvature relationship for a section at the base of the wall. The lateral load

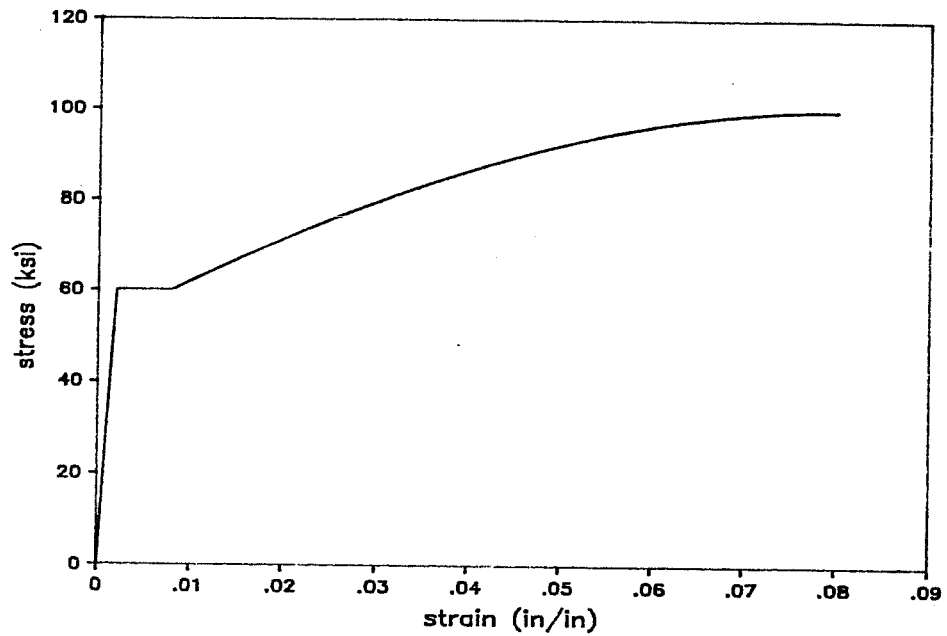


Figure 4.8 Steel Strain-Stress Relationship Used in RCCOLA

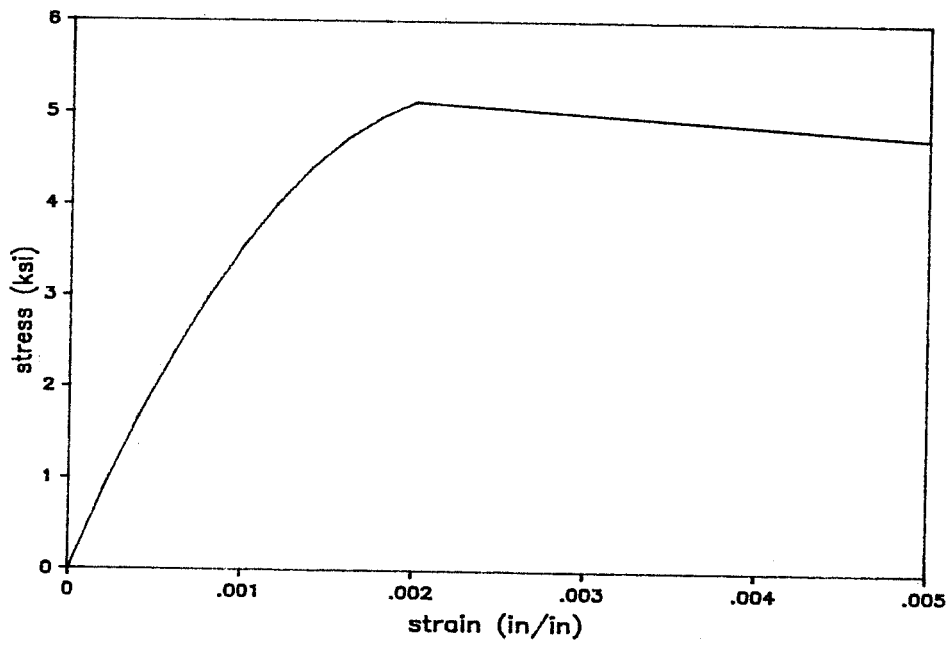


Figure 4.9 Concrete Strain-Stress Relationship Used in RCCOLA

associated with the moment at first yield was $V_{my} = 291$ kips. ($M_y = 36732$ kip-in.). First yield was reached at a load of 276 kips. The use of RCCOLA provided a good estimate, overestimating the test value by only 5%.

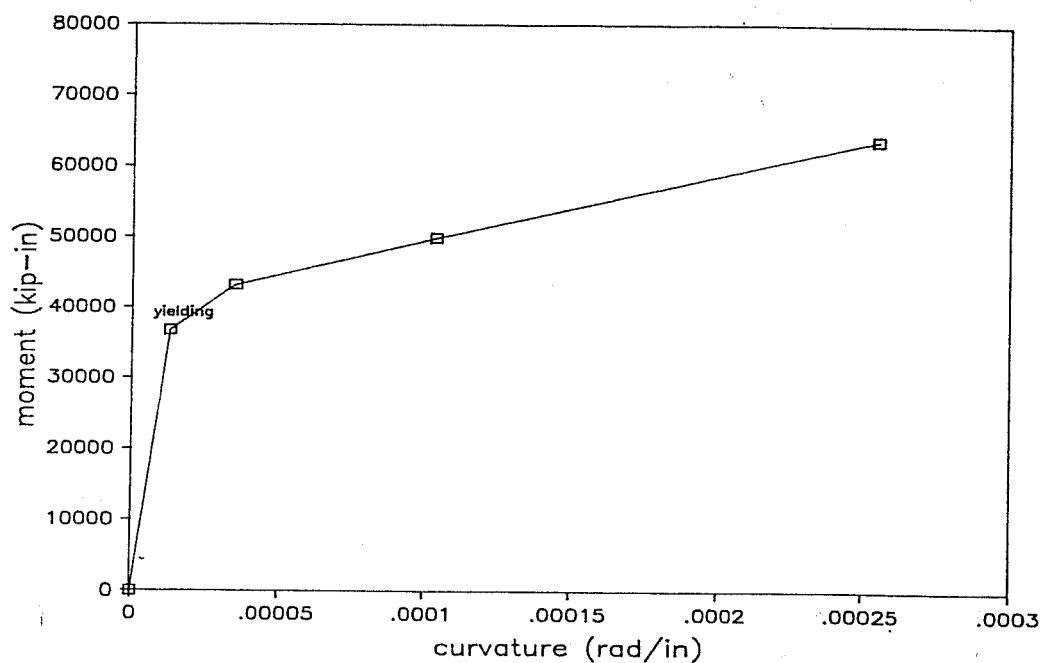


Figure 4.10 RCCOLA Moment-Curvature Relationship

Maximum strength predicted using RCCOLA was 505 kips, 23% higher than the peak load (410 kips) reached at the end of the test.

4.3.3 Shear Strength. The maximum shear strength was estimated using the current provisions in Appendix A of ACI 318-86, where the shear strength is given by the formula:

$$V_n = A_{cv}(\alpha_c \sqrt{f'_c} + \rho_n f_y) \quad (7)$$

where

A_{cv} = net section area of the wall web.

ρ_n = ratio of distributed shear reinforcement on a plane perpendicular to A_{cv} .

$f_y =$ yield strength of reinforcement steel.

$\alpha_c =$ coefficient which defines the relative contribution of the concrete (function of the aspect ratio).

Using a 1.67 aspect ratio in equation (7), leads to a maximum shear strength of 365 kips ($6.0 \sqrt{f'_c} bd$), indicating that provisions of ACI 318-86 result in underestimating the shear strength of the specimen. It is believed that the difference between the test and the code estimation exists because the code neglects the added area of concrete and longitudinal reinforcement in the boundary elements, the strain hardening of the wall reinforcement, and the effect of the top beam (or floor slab in a real structure) in restraining the opening and extension of shear cracks. Code procedures would be expected to yield more conservative estimates of strength for elements failing in a brittle manner. A better estimation may be achieved through design suggestions obtained in similar tests conducted by Barda, Hanson and Corley [8]. Maximum strength predicted using Reference [8] was $9.26 \sqrt{f'_c}$, compared to the $6.84 \sqrt{f'_c}$ reached at the end of the test. A summary of the strength calculated by the methods discussed above is listed in Table 4.1.

Table 4.1
Strength Evaluation

First Cracking	Flexural Capacity
$V_{cr} = 268$ kips $V_{crexp} = 120$ kips	$V_{aci} = 394$ kips $V_{rccola} = 505$ kips $V_{maxexp} = 410$ kips
First yield $V_{fyrecola} = 291$ kips $V_{fyexp} = 276$ kips	Shear Capacity $V_{aci} = 365$ kips $V_{maxexp} = 410$ kips

4.3.4 Splice Design. The length of the splice for the flexural reinforcement in the existing frame columns was dictated by provisions in the 1955 edition of the Uniform Building Code. Splice lengths were a function of the working compression stress of the bar and were specified in terms of the bar diameter for a minimum concrete strength of 3000 psi. The resulting length of the lap splice was 24 bar diameters, or 21 in. for a #7 bar. The current design requirements, considering tension due to the overturning moment, for the same splice condition is 39 in.. The difference reflects the inadequacy of the original detail to develop full strength of the bars.

The purpose of adding the reinforced concrete jackets to the existing columns was to improve the performance of the tension splice. A new analysis was made following the current guidelines of ACI committee 408 [4]. Considering the concrete cover and the confining reinforcement in the boundary elements, it was found that a 17 in. lap splice was needed (80% of the length provided).

The performance of the splice was satisfactory. Strains measured in the spliced bars reached values 6.5 times the yield strain. No indication of splice failure (splitting) was observed from cracking of the concrete surface in the splice region.

4.4 Energy Dissipation Capacity

The energy dissipated by the specimen refers to the area within the load-deflection hysteresis loops. The energy is computed from the load-displacement history. Figure 4.11 shows the energy dissipated per cycle vs drift. Figure 4.12 shows the drift versus energy dissipated normalized with aspect to the peak displacement variation per cycle. If the specimen had an ideal elasto-plastic response without deterioration as drift increased, the normalized values in Figure 4.13 would be constant. A drop in the curve shown in Figure 4.12 reflects pinching of the hysteresis loop or loss of energy absorption capacity.

The specimen showed a steady gain of energy absorbing capacity with increments of drift. Some deterioration was observed when the specimen was loaded to repetitive cycles to 0.23% drift (cycles 9,10 and 11) even when the load reached was virtually the same. As the drift increased, the energy dissipation capacity increased as the flexural steel began strain hardening.

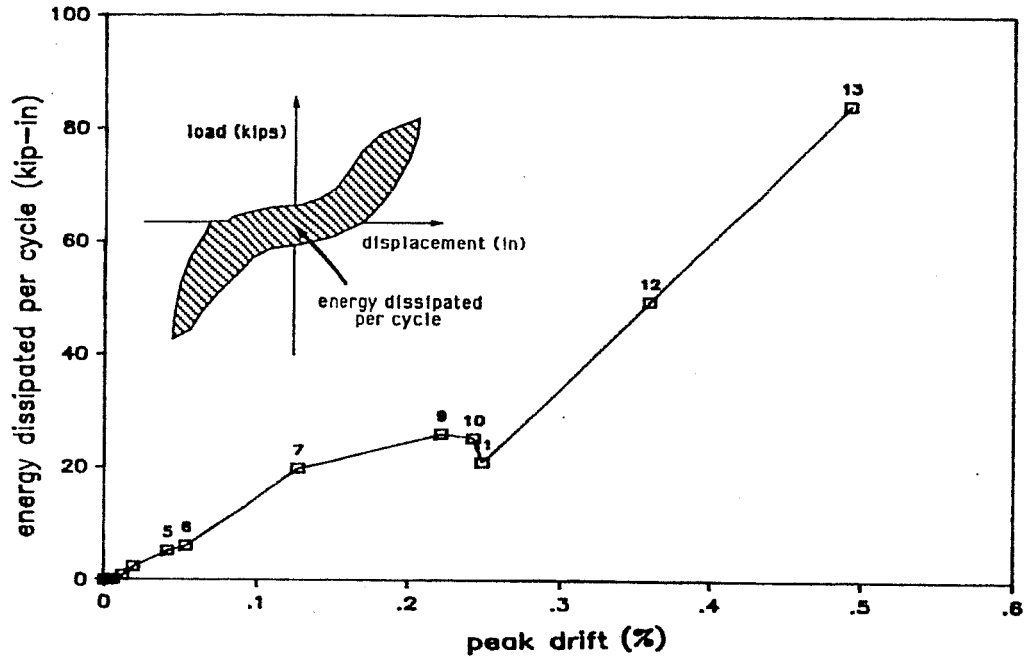


Figure 4.11 Energy Dissipation in Each Cycle vs. Drift

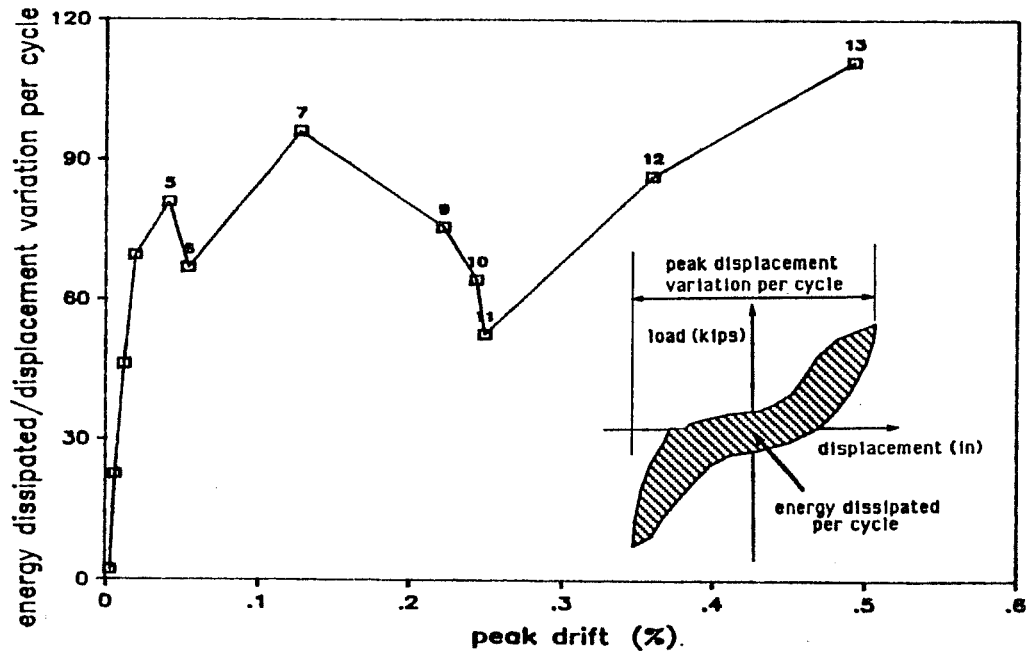


Figure 4.12 Normalized Energy Dissipated on Each Cycle

4.5 Comparison of Eccentric Wall to Infill Wall

The most significant differences in the response of the eccentric wall and the infill wall tested by Gaynor [1] are:

- a) The eccentric wall showed a higher strength than the infill wall at every level of drift. Maximum load applied to the eccentric wall was 410 kips, compared to a failure load of 271 kips for the infill wall. Figure 4.13 shows the load versus drift envelopes for the two specimens.
- b) The flexural reinforcement in the existing frame columns of the eccentric wall developed up to 6.5 times the yield strain without indicating splice failure. The infill wall failed at the column splice developing only 70% of the yield strain.
- c) Even though the existing columns in the eccentric wall specimen were cracked before the test began, its stiffness was higher and the degradation more gradual than that of the infill wall from the beginning to 0.1% drift cycle. After 0.1% drift cycle, the measured stiffness normalized with respect to the theoretical elastic stiffness were about the same in both tests. Figure 4.14 shows the load versus normalized stiffness for the two specimens.
- d) Energy absorption capacity of the eccentric wall was higher than that of the infill wall. Figures 4.15 and 4.16 show that the infill wall not only deteriorated more for repetitive cycles but that the energy dissipated was also less as the drift increased.
- e) The compression struts in the eccentric wall extended diagonally from the very top corner of the wall to the bottom of the download column. Compression struts in the infill extended within the infill panel, creating concentrations of shear stresses at the bottom and top of the boundary members.
- f) The transfer of shear from the existing frame to the eccentric wall was achieved with virtually no slip between surfaces. The infill wall test showed up to 0.03 in.(6% of the lateral displacement) of relative slip between the top beam and the infill wall.

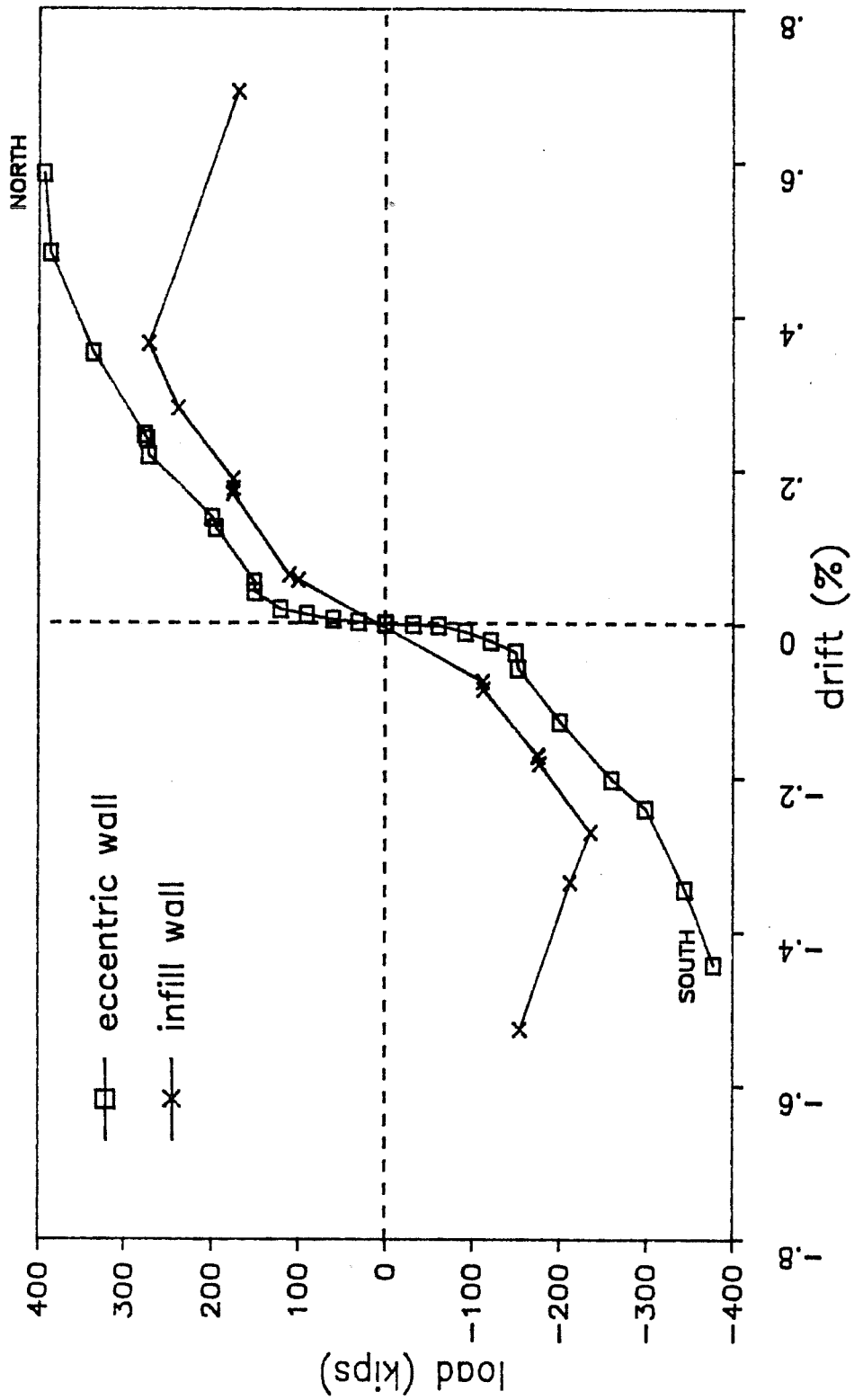


Figure 4.13 Load vs. Drift Envelopes

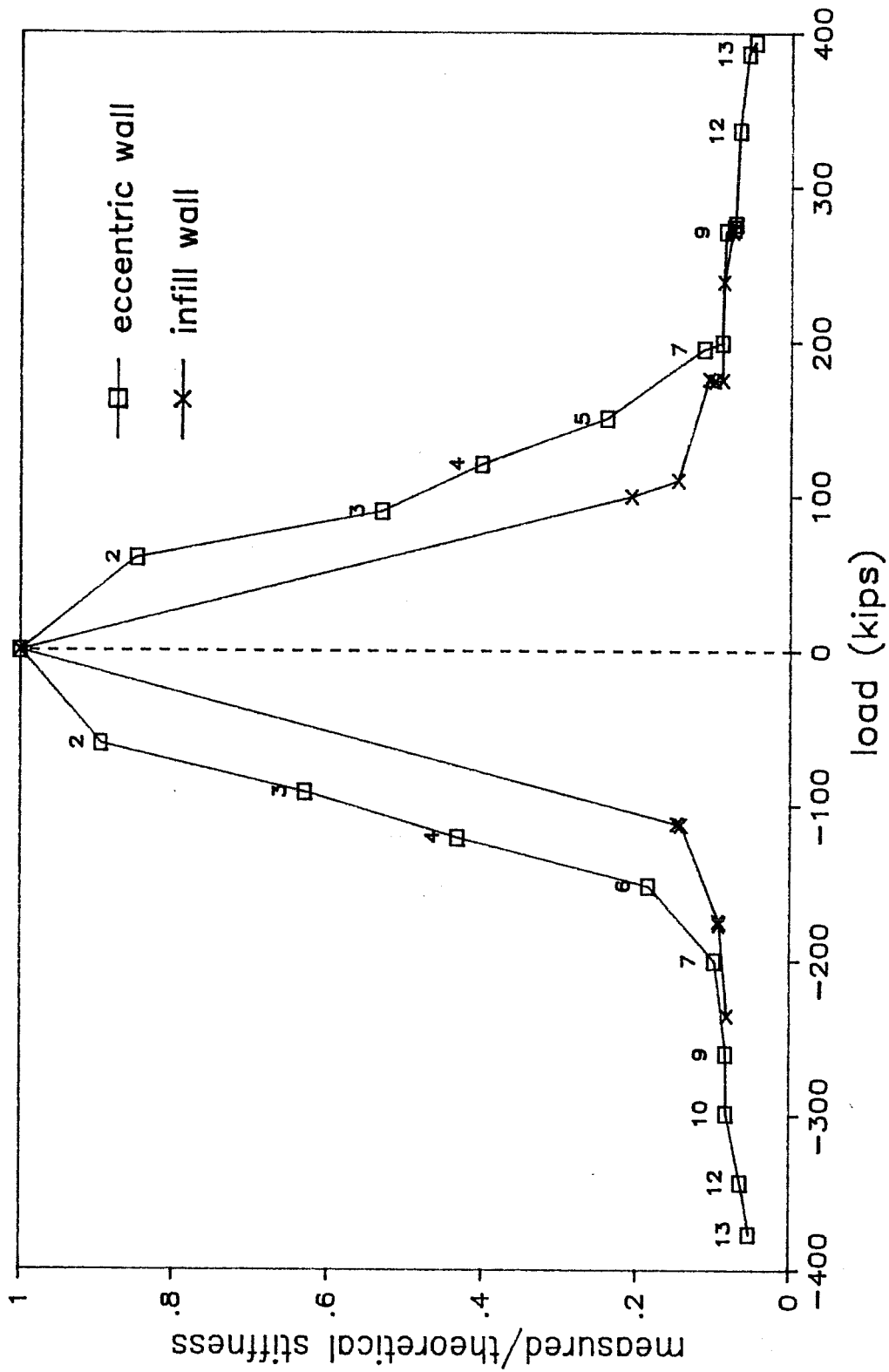


Figure 4.14 Load vs. Normalized Stiffness

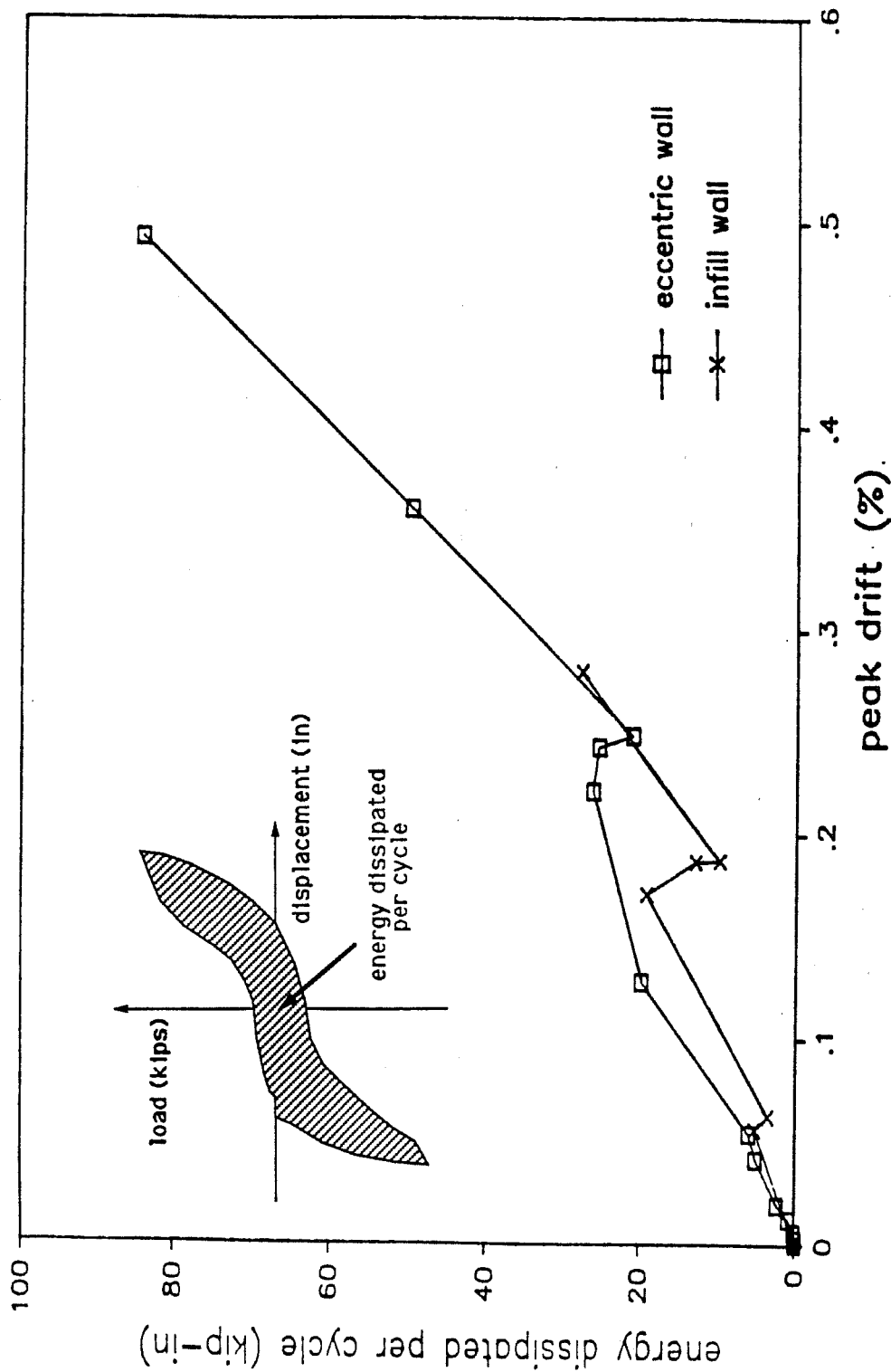


Figure 4.15 Energy Dissipated Per Cycle

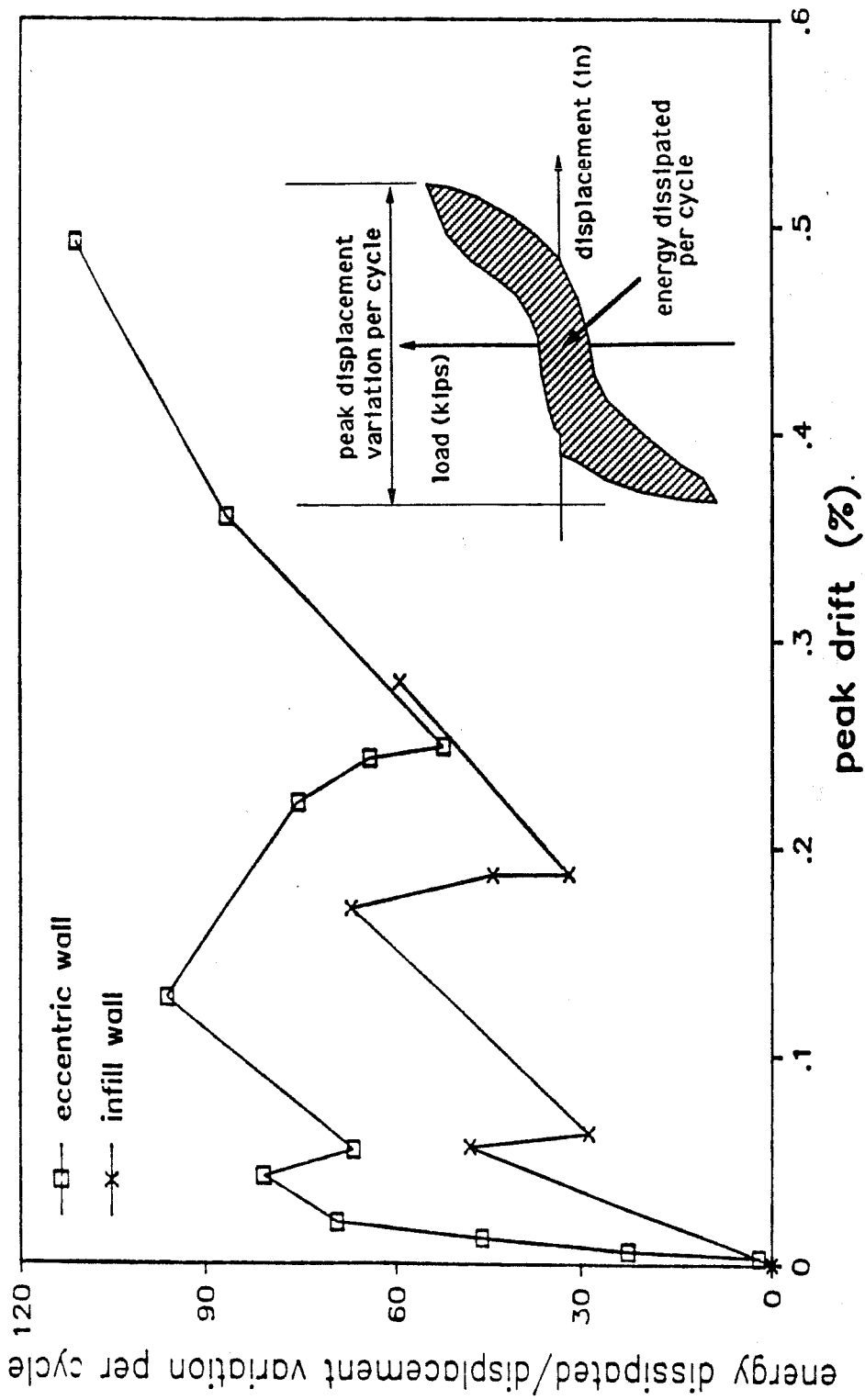


Figure 4.16 Normalized Energy Dissipated in Each Cycle for Eccentric and Infill Walls

CHAPTER 5

SUMMARY, CONCLUSIONS AND RESEARCH RECOMMENDATIONS

5.1 Summary

The performance of a non-ductile reinforced concrete frame strengthened with a reinforced concrete wall designed to carry inplane lateral cyclic loads was investigated. A two-third scale model was built and tested. The reinforced concrete frame was representative of 1950's construction in seismic areas. The frame columns had a compression splice at the base of the columns. In previous tests, a splice failure occurred in the columns when the boundary element was in tension. The splice failure limited the capacity of the strengthened frame system. In the current test, the concrete wall was eccentric to the plane of the frame. It was connected to the concrete frame through epoxy grouted dowels and reinforced concrete jackets around the frame columns and was faced against the outside of the columns. The jackets improved the behavior of the column splice, allowing steel strains well beyond yield without failing. When loading was stopped, a well distributed pattern of cracking (flexural and shear) was observed. The capacity of the test structure exceeded the capacity of the loading system. The vertical wall and column reinforcement at the base was well into the yield range and the load- deflection curve was nearly flat indicating that the ultimate load in flexure was almost reached.

5.2 Conclusions

1. The theoretical flexural and shear capacity predicted by ACI 318-86 were conservative for the tested specimen. It was observed that the new and existing concrete acted monolithically. For this test, the monolithic action assumed in the design of the eccentric wall was verified by the results.
2. Failure of the frame column splice was successfully avoided by using a thicker concrete cover and additional transverse reinforcement. Up to 6.5 times the yield strain was developed in the spliced bars.
3. Reinforced concrete frames strengthened with an eccentric wall and column jackets performed better (strength, stiffness, and energy dissipation capacity) than similar frames strengthened with an infill wall.

4. Negligible slip was observed between the reinforced concrete frame and the eccentric wall.
5. Epoxy grouted dowels developed very low strains. It is likely that most of the shear was transferred through the column jackets.
6. Strains in the transverse reinforcement in the column jackets were low. The transverse reinforcement required by Appendix A of the ACI 318- 86 was conservative for the eccentric wall.
7. The specimen reached yield before it reached a drift ratio of 0.005%, an index used in the Uniform Building Code.
8. The out-of-plane displacement due to the torsion created by the eccentricity of the wall did not appear to affect the response of the specimen. The only indication that torsion was present were a few diagonal cracks on the inside face of the column.

5.3 Research Recommendations

1. The effectiveness of epoxy grouted dowels to transfer shear forces from the existing frame to the strengthening element is not clear. If an alternative path, as in the case of column jackets, is available to transfer the entire load, the use of epoxy grouted dowels would not be necessary, thus eliminating extra handling and placing that epoxy requires.
2. Measured strains in the jacket transverse reinforcement were small. The possibility of using smaller size bars and/or larger spacing than the test transverse reinforcement would simplify the construction of the column jacket.

REFERENCES

1. Gaynor, P. J., "The Effect of Openings on the Cyclic Behavior of Reinforced Concrete Shear Walls", Master's Thesis, The University of Texas at Austin, May 1988.
2. Shah, S. N., "Evaluation of Infill Wall Strengthening Schemes for Non-Ductile Reinforced Concrete Buildings", Master's Thesis, The University of Texas at Austin, May 1989.
3. American Concrete Institute, "Committee 318, Building Code Requirements for Reinforced Concrete (ACI 318-86)", American Concrete Institute, Detroit, 1986.
4. American Concrete Institute, Committee 408, "Suggested Development, Splice, and Standard Hook Provisions for Deformed Bars in Tension" (Report No ACI 408.1R/79), Concrete International, Vol 1, No 7, July 1979, pp 44-46.
5. Farahary, M. M., "Computer Analysis of Reinforced Concrete Cross Sections", Master's Thesis, The University of Texas at Austin, December 1983.
6. International Conference of Building Officials, "Uniform Building Code", 1955 Edition, Whittier, California, 1955.
7. Scott, B. D., Park, R., and Priestley, M. J. N., "Strain-Stress Behavior of Concrete Confined by Overlapping Hoops at Low and High Strain Rates", ACI Journal, January-February 1982, pp 13-25.
8. Barda, F., Hanson, J. M., and Corley, W. G., "Shear Strength of Low-Rise Walls with Boundary Elements", Reinforced Concrete Structures in Seismic Zones, American Concrete Institute, Publication SP-53, pp 149-202.
9. Hiraishi, H., "Evaluation of Shear and Flexural Deformations of Flexural Type Shear Walls", Bulletin of The New Zealand National Society for Earthquake Engineering, Vol 17, No 2, June 1984, pp 135-144.
10. Vallenias, J. M., Bertero, V. V., and Popov, E. P., "Hysteretic Behavior of Reinforced Concrete Structural Walls", Report No UCB/EERC-79/20, Earthquake Engineering Research Center, University of California, Berkeley, August 1979.

11. Kahn, L. F., "Reinforced Concrete Infill Walls for Aseismic Strengthening", Ph.D. Thesis, University Of Michigan, Ann Arbor, Michigan, 1976.
12. Sugano, S., and Fujimura, M., "Aseismic Strengthening of Existing Reinforced Concrete Buildings", Seventh World Conference on Earthquake Engineering, Part I, V4, Istanbul, Turkey, 1980, pp 449-458.
13. Bett, B. J., "Behavior of Strengthened and/or Repaired Reinforced Concrete Columns Under Reversed Cyclic Deformations", Master's Thesis, The University of Texas at Austin, May 1984.
14. Bass, R. A., "An Evaluation of The Interface Shear Capacity of Techniques Used in Repair and Strengthening of Reinforced Concrete Structures", Master's Thesis, The University of Texas at Austin, August 1984.
15. Roach, C. E., "Seismic Strengthening of a Reinforced Concrete Frame Using Reinforced Concrete Piers", Master's Thesis, The University of Texas at Austin, May 1986.
16. Degenkolb, H. J., and Associates, "Repair and Strengthening of Reinforced Concrete Structures", San Francisco, March 1983.

VITA

Larry Roland Jimenez Pasquier was born in Masaya, Nicaragua, on December 8 of 1960. The second son of Lesbia A. Pasquier Hueck and Rolando J. Jimenez Vallejos. He received his High School Diploma from Colegio Calasanz, San Jose, Costa Rica, in 1978. He enrolled The School of Engineering at the University of Costa Rica, San Jose, Costa Rica, in 1979. He graduated from The University of Costa Rica with a "Licenciatura" degree in Civil Engineering in August of 1984. He entered The Graduate School at The University of Texas at Austin in January of 1987.

Permanent address: Apartado 8552-1000
San Jose, Costa Rica

This thesis was typed by Larry Jimenez.

*A ti Señor Creador,
a ti padre y madre
por darme vida y fortaleza*